Impact of Cyber Failures on Operation and Adequacy of Multi-Microgrid Distribution Systems

Mostafa Barani[a,*], Vijay Venu Vadlamudi[a], Hossein Farzin[b]

[a]*Department of Electric Power Engineering, Norwegian University of Science and Technology (NTNU), Trondheim, Norway*
[b]*Faculty of Engineering, Department of Electrical Engineering, Shahid Chamran University of Ahvaz, Ahvaz, Iran*

Abstract

The primary objective of this paper is to create a suitable reliability assessment framework for Cyber-Physical Multi-MicroGrid (CPMMG) distribution systems, considering device-level failures of control and protection systems. For this purpose, the typical structure of a CPMMG distribution system with a centralized protection system is first exemplified. Then, the interdependencies between cyber and power infrastructures are investigated in such systems. Regarding the protection system, a Markov model is presented to investigate hidden failures of fault location, isolation, and service restoration processes. Possible operation modes in a CPMMG distribution system—normal, islanding, joint, and shutdown modes—are then explained and modeled. Finally, a suitable Monte Carlo simulation-based reliability assessment framework is developed to quantify well-known reliability indices. In addition, two new adequacy indices are proposed: Interrupted but Gained Compensation (IbGC) and Supplied by Expensive Resources (SbER). A comprehensive case study is conducted to reveal the salient features of the proposed framework. The result showed that the impact of cyber failures in such systems is highly dependent on the design of the cyber system. Therefore, the adverse impact of cyber failures of control and protection systems can be effectively mitigated by proper design.

Keywords: multi-microgrid, adequacy, information and communication technology, cyber system, reliability, distribution systems.

---

*Corresponding author
Email address:* `mostafa.barani@ntnu.no` (Mostafa Barani)

List of Acronyms

CBC	Circuit Breaker Controller
CPDS	Cyber-Physical Distribution System
CPMMG	Cyber-Physical Multi-MicroGrid
CPPS	Cyber-Physical Power System
IbGC	Interrupted but Gained Compensation
ICT	Information and Communication Technology
DER	Distributed Energy Resource
EENS	Expected Energy Not Supplied
ESS	Energy Storage System
FLISR	Fault Location, Isolation, and Service Restoration
FO	Fiber Optic
HEMS	Home Energy Management System
IO	Islanding Operation
JO	Joint Operation
LC	Load Controllers
MC	Micro Controller
MCS	Monte Carlo Simulation
MG	Microgrid
MGCC	Microgrid Control Centers
MMG	Multi-MicroGrid
NO	Normal Operation
POI	Point of Interconnection
PS	Proportional Shares
SbER	Supplied by Expensive Resources
SMCS	Sequential Monte Carlo Simulation
SOC	State of Charge
SW	Network Switch

1. Introduction

1.1. Motivation & Scope

Integrating Information and Communication Technologies (ICTs) into physical, engineered systems has given rise to cyber-physical systems [1]. As one particular case, with the rapid evolution of the ICTs and the automation of system control, the ICTs have gradually become an integral part of the power systems [2], to the context that the resulting system is so-called Cyber-Physical Power

Systems (CPPS). In these systems, ICTs take the center stage in improving the performance of the power systems across various aspects by automation of system control and monitoring, peer-to-peer communication, and data gathering & processing [3, 4]. With all the benefits that ICT deployment brings to CPPSs, failure of these can deteriorate the functionality of the CPPSs. The adequacy of a CPPS is also not an exception; therefore, it is affected by the failure of ICTs. Although the impact that the failure of ICT components exerts on CPPS adequacy is not as vast as the failure of power components themselves, it is vital to investigate their impact to design a more efficient system. The reliability of CPPSs, similar to the reliability of the power systems, can be separately assessed at different functional zones, i.e., generation, transmission, and distribution levels, of which the latest one is of interest—within the scope—of this study.

1.2. Background Knowledge

The past decade has seen the gradual development of both simulation-based and analytical approaches for studying the adequacy, and thus the reliability, of Cyber-Physical Distribution Systems (CPDSs). Failure of a cyber component, based on the component's function, can impact the operation of the power system *directly* (where it has a primary function, such as controlling a generation unit) and *indirectly* (where it has a secondary task, such as controlling a power switch for isolating a faulted zone) [5, 6]. There has been a focus on modeling various existing interdependencies and quantifying the impact of cyber system failures on the performance of CPDSs. As one of the first attempts, Bamdad *et al.* developed two methods based on state enumeration, state mapping, and state updating to investigate these direct and indirect impacts on a smart grid [3, 7]. References [8, 9] used the same methods and further developed these studies by incorporating the volatile nature of wind generation into the assessment. Similarly, Hashemi *et al.* developed two frameworks based on Monte Carlo Simulation (MCS) by incorporating uncertainties of renewable generations and loads for evaluating these direct and indirect impacts [10, 11]. Reference [12] introduced an analytical method based on the complex network theory to assess the risk of smart grid failure due to the communication network malfunction associated with latency and ICT network reliability. Cao *et al.* further studied the impact of over-voltage issues on the reliability in active distribution networks caused by cyber contingencies [13]. Several studies also investigated the indirect impact of cyber failures on the reliability of CPDSs, with a focus on cyber components involved in the protection and restoration of the system. Liu *et al.* evolved the design of the required cyber system and investigated the impact of cyber failures on system protection and restoration based on non-sequential and Sequential MCS (SMCS), with a focus on validity evaluation of the cyber links [14]. They subsequently proposed an analytical method by combining the minimal path set method and frequency-time domain transformation for the same purpose [15]. This study was further evolved in [16] by adding more detail to power switch controllers. Reference [17] recently proposed an analytical approach based on an

3

anticipated fault set to analyze the impact of cyber system failures on protection systems.

In parallel, several studies have been carried out to assess the impact of cyber component failures on the adequacy of isolated Microgrids (MGs) [18, 19, 20, 21, 22]. For this purpose, reference [18] developed an MCS-based method to investigate the impact of cyber system failures and disturbances on isolated MGs; reference [19] evolved this study by adding optimization-based scheduling strategies to the model; references [20, 21] further developed these studies by taking the uncertainty of Distributed Energy Resources (DERs) and loads into account. Reference [22] recently developed a framework by integrating an information mapping model into the state transition of a physical MG to quantify the impact of cyber system contingencies on MGs. All these studies are only applicable to isolated MGs. We recently developed a framework based on SMCS to analyze the impact of cyber components failure on single grid-connected MGs [23].

1.3. Research Gap Identification & Research Contribution

MGs have limited energy handling capability. According to IEEE recommendations, the maximum capacity of MGs is normally limited to 10 MVA [24]. In this regard, a distribution network can be partitioned into a number of MGs [25]. In recent years, this has led to the idea of Multi-MicroGrid (MMG) systems, which are formed by connecting adjacent MGs to enhance the operation and control of the system [26]. Despite the greater penetration of ICTs in Cyber-Physical MMGs (CPMMGs), less attention has been devoted to these systems in the literature. The main objective of this paper is to fill this gap by proposing a framework based on SMCS for the adequacy assessment of CPMMG distribution systems, taking into account the device-level failures in the control and protection systems of CPMMGs. Although the main research question that motivated us to conduct this work was to investigate the impact of device-level cyber failures in CPMMGs, we faced two more research questions during this study. The first research question was: "What is a suitable method for treating the uncertainty associated with the duration of contingencies in the scheduling of the system?". The second research question was: "How does moving toward privatization of power systems and the appearance of new actors influence the system reliability?" Solutions for these two research questions related to CPMMGs are also offered in this paper. The contributions of this paper are as follows:

- A cyber structure suitable for a CPMMG is exemplified; relevant direct and indirect interdependencies between the cyber components involved in *control* and *Fault Location, Isolation, and Service Restoration (FLISR)* systems, and the power components in a CPMMG system are identified; and the consequences are analyzed. Since no study has simultaneously studied the impact of cyber component failures in both the control system and FLISR on distribution system adequacy, these two are explained separately for clarity. Regarding the control system, non of the aforementioned studies on CPDSs included MGs in their studies. The inclusion of MGs and MMGs

4

in the distribution networks requires additional control layers (i.e., the Microgrid Control Centers (MGCCs)) that in turn change the required cyber infrastructure; the interdependencies between cyber and power components change accordingly. This paper incorporates these control layers and their connections into account. The load controllers in this study are also modeled as having an indirect impact, which has not been considered in previous studies. Regarding the impact of cyber component failures on FLISR, several studies have been conducted. Two of the most comprehensive studies ([14, 16]) that encompass all aspects of other studies are compared with this work. Compared to the first study [14], a detailed cyber system for the power switches is considered, including actuators and sensors. Compared to the second study, this paper evaluates the impact of power switch operation on tasks other than protection, such as the successful islanding of MGs. Compared to both studies, a Markov model that can be used aligned with SMCS is presented to incorporate hidden failures and components' inspection based on a predefined schedule into the SMCS technique. The uncertainty regarding the manual switching times is also considered in this paper.

- An SMCS-based framework that performs a cyber-power joint analysis is developed to assess the impact of control and protection systems' failure on the adequacy of CPMMG systems that include resources with temporal correlation.

- Based on the contingency states in the system (which are obtained using SMCS), scheduling strategies with a focus on load modeling and component failures that are simplified but suitable for acquiring adequacy indices have been developed to characterize the system behavior during various operation modes, namely normal, islanding, and joint operation modes. It also includes a generic approach for dealing with the uncertainty associated with the repair times of failed components that can be adopted by scheduling strategies used in practice.

- Due to the restructuring of the power system, the ownership of different parts of a power system may matter in the adequacy assessment. We have raised this issue for an MMG system. During joint operations, where some MGs are connected to each other but separated from the upstream grid, MGs with cheaper loads might interrupt their loads and sell energy to other MGs that require this energy to supply their more expensive loads. While this load interruption and transaction must benefit both parties, it was considered the interrupted load for the seller MGs in conventional adequacy indices. In this regard, two new adequacy indices—Interrupted but Gained Compensation (IbGC) & Supplied by Expensive Resources (SbER)—are proposed to capture these transactions in MMG systems, which is necessary for studying self-interested MGs in an MMG distribution network.

The remainder of the paper is organized into five sections: Section 2 exemplifies the structure of a CPMMG, and the consequences of failure of various cyber components are determined. Section 3 presents three mathematical formulation problems for the scheduling strategies of an MMG during normal, islanding, and joint operation modes. Section 4 explains the proposed methodology for obtaining adequacy indices. Section 5 provides the results of the case study. Finally, Section 6 concludes the paper.

2. System and Component Description

2.1. Cyber-Physical Multi-Microgrid Systems

Figure 1 shows the structure of a sample CPMMG system. This cyber structure includes three control layers: 1) the Distribution Management System (DMS), 2) the MG Control Center (MGCCs), and 3) the primary controllers. The primary controllers include Micro Controllers (MCs) for controlling DERs, viz., wind, PV, ESS, and diesel engine units; Load Controllers (LCs); and Circuit Breaker Controllers (CBCs). The LCs are considered to control the bulk load points that, for example, might encompass several residential customers, each of whom is equipped with a Home Energy Management System (HEMS). The controllers at different layers are connected through communication layers, which can be implemented using wired or wireless communication technologies. Note that the physical MGs are connected to each other at Points of Interconnection (POIs).

2.2. Availability of Cyber Links

A cyber link between two cyber components is available if at least one cyber route for transferring data between them is available. The *structure function* in the form of minimal *sum-of-products* is used to find the availability of the cyber links [23]. The minimal path sets—that include all cyber components in a communication route—required in this method can be efficiently found using the adjacency matrix of the fully operational cyber system in different programming languages, such as in MATLAB by using the command '*allpaths*'. Note that in this paper, a cyber (communication) route refers to a single communication path between two cyber components, and a cyber link refers to all possible communication paths between two cyber components.

2.3. Impact of Cyber Component Failures

In order to study the impact of the failure of cyber components, the first step is to identify possible failure events and their consequences. Unlike the failure of power components, a general formula is not feasible for identifying the consequences of cyber component failures which depend on the design and logic of the control systems, the function of cyber components, in addition to the structure of the cyber network. For instance, a centralized control system is prone to a single
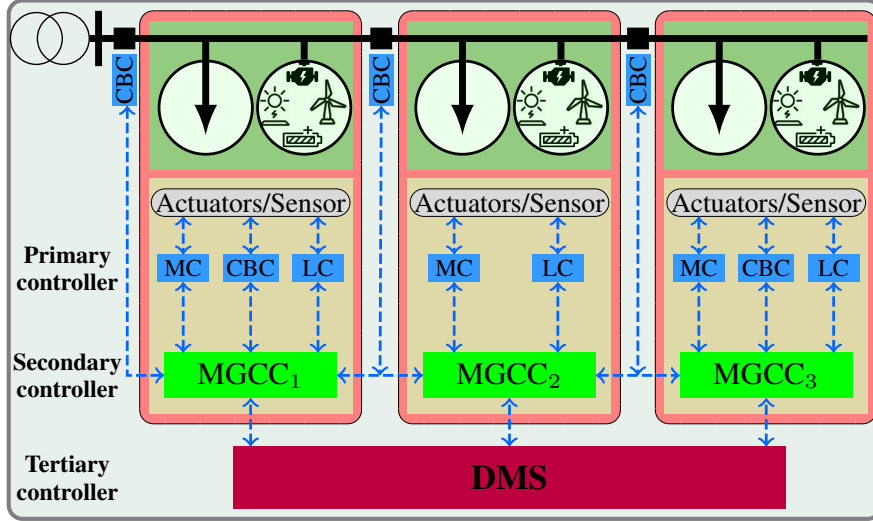
Figure 1: Schematic architecture of a CPMMG system.

point failure, and when it is down, the whole system under its control will be down; however, for a distributed control system, this is incorrect.

This study considers centralized controllers at both the MMG (DMS) and MG (MGCCs) levels. The DMS coordinates MGs to maintain the economy and security of the distribution network [27]. Therefore, its failure results in the separation of the distribution network from the upstream network and the shift of the MGs to islanding mode. An MGCC is the core of the MG control system, and with its failure, MG shuts down [20]. As the DMS handles coordination among MGs, if an MG loses its communication link to the DMS, it shifts to island mode, and the MGCC is solely responsible for the operation of the MG. The LCs gather the data of the bulk load points at each distribution node and are responsible for the interruption or shifting of the loads when required. In this regard, when it fails, the load point under its control cannot be interrupted. Commands are also issued from the MGCCs to these LCs. Therefore, the failure of a cyber link between an MGCC and a load controller also results in an uninterruptible load point. This has an indirect impact on the system. Furthermore, the failure of an MC (controller of a DER) or its cyber link to the corresponding MGCC result in the outage of the related unit. Distribution networks might be able to maintain their normal operation when they lose their communication channel to the upstream network. On the other hand, with the increasing penetration of DERs in the distribution networks, exchanging information between the DMS and the upstream network might become necessary for the safe operation of these systems. In this regard, both these assumptions are evaluated in the case studies. As discussed earlier, the consequence of the failure of cyber components in the control system of a CPMMG depends on the logic of the control system. This section considered a probable scenario for the consequence of failure of cyber components in the CPMMG under study.

As another logic, for example, if the DMS and MGCCs experience a malfunction, the correspond-

ing section of the system they oversee can transition into a passive mode. This transition involves disconnecting all active resources, including generation resources. Under this logic, the upstream network is responsible for providing power to all loads in the distribution network. As a result, failures within the control system have minimal influence on the Expected Energy Not Supplied (EENS) index, rendering its calculation less meaningful in this case. The outcome closely aligns with the values reported for the distributed control system in section 5.4.2. Alternatively, it may be more informative to calculate the Expected Energy Not Produced (EENP) to assess the impact of control system failure. This metric would provide insights into the amount of energy that would go ungenerated due to such failures. This study has employed the logic explained earlier to assess the maximum impact of component failures within the control system and explore potential strategies for mitigating their effects.

2.4. Fault Location, Isolation, and Service Restoration

The decision model in protection systems can adopt local, distributed, or centralized schemes. In the local scheme, the local controller of each power switch is responsible for the operation of the related power switch. In the distributed layout, the controller of the power switches together with the communication between themselves allocates the decision-making process. In this study, a centralized protection system (under MGCCs and DMS control) was considered for two reasons. First, centralized protection requires higher integration of ICTs. More importantly, with the high penetration of DERs into a distribution system, which is the case in this paper, the protection system becomes a concern. Centralized protection schemes can resolve this concern and many other protection limitations [28, 29]. Due to the wide range of designs for the protection and restoration processes, the following assumptions are made for the operation of the power switches:

- **Assumption 1:** Only the central processor of the protection system issues open and close command signals, and there is no local setting for the power switches.

- **Assumption 2:** All the power switches in this study can disconnect under the load. We only calculated the EENS adequacy index in this study. Due to the very small switching time in an automated protection system, this assumption's impact on the adequacy index EENS is very negligible, and it hardly influences the results. If frequency indices are to be calculated, consideration of power switches that cannot operate under load may impact the results. However, in such cases, this assumption can be easily relaxed.

- **Assumption 3:** Only the data of the sensors of the power switches that surround a faulted zone can determine the faulted area. As there might be several other sensors in a CPMMG distribution network, for example, at the point of interconnections of DERs, more comprehensive approaches may be feasible for fault location. The impact of each specific algorithm and approach should be
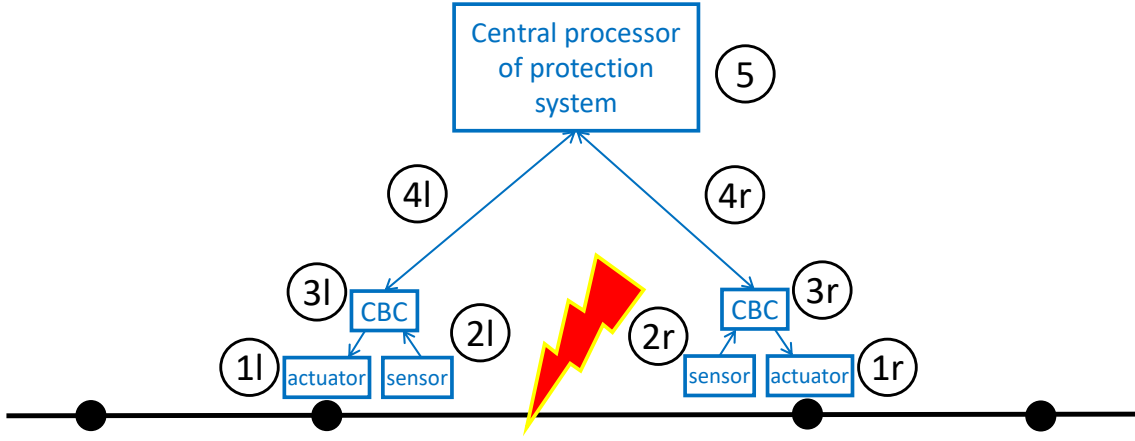
Figure 2: FLISR with a centralized decision-making scheme.

evaluated separately, and this assumption is necessary here. Nevertheless, it only impacts fault location identification.

Consider the protection system shown in Figure 2 with the aforementioned assumptions. In such a system, the measurements are taken by the sensors and then the information is collected by the CBCs and transferred to the central processor through the CBC's communication module and the corresponding cyber link. Afterward, the central processor, according to the received information, determines the fault location and issues the necessary command signals. Thereafter, these command signals are sent to the related power switches via the communication system. The actuators finally execute the commands and isolate the faulted area. Finally, the execution confirmation signals are sent back to the central processor. If possible, the relevant commands are also issued for maximum service restoration in the system by benefiting from an islanding operation or available tie switches. With the failure of the central processor, the entire automation system is down. Assuming that the central processor is properly working, the rest of the failures are elaborated on in the following:

2.4.1. Fault Location

As per the aforementioned explanation, the first step toward fault clearance is the determination of the fault location. With the shown fault in Figure 2, the proper operation of the corresponding sensors (2l and 2r), CBCs with built-in communication modules (3l and 3r), and the cyber links for transferring the data to the central processor (4l and 4r) are necessary to properly identify the fault location provided that the central processor of the protection system is operational. Failure of any of the mentioned components results in the lack of acquired information by the central processor, which causes the extension of the faulted area. For example, the failure of 2r, 3r, or 4r results in the expansion of the isolated area to the right-hand side of the faulted zone. In this case, the information received from the first neighboring power switch with fully working cyber components

will be used instead. Keep in mind that, in this case, the location of the fault is not known by the central processors. This point is important if manual switching is feasible.

2.4.2. Fault Isolation

After identifying the fault location, the central processor issues the command for opening the corresponding power switches to isolate the faulted zone and necessary commands to the corresponding switches for system restoration. To isolate the faulted area properly, the operation of the corresponding cyber link, the power switch controller that includes the communication module, and the actuators for executing the open command of the power switches are required. Failure of any of these components results in the mis-operation of the power switches. Since the corresponding cyber link and the CBC have been involved in the fault location process, issuing a command signal for opening a power switch means that the corresponding cyber link and CBC are already working. If the switch cannot operate as a result of the failure of the actuator, the control center will send a command signal to the closest power switch to isolate the faulted zone. This causes the extension of the fault to a neighboring area. If manual switching is available, the non-faulted area can be diminished by manual switching. In this case, the decisions regarding manual switching can be immediately made. Comparing this case with the fault location process, it is expected to have a smaller manual switching time because the switches that should operate are already known in this case.

2.4.3. Service Restoration

The elements required for proper service restoration are the same as those required for fault isolation. These elements are the corresponding cyber link, the power switch controller, which includes the communication module, and the actuators for executing the open/close commands. With the failure of any of these components, automatic service restoration cannot be carried out. If manual switching is available, the switching time will be the same as the one explained in section 2.4.2, since the power switches that should operate are also already known in this case.

2.4.4. Modeling of the Failure and Repair Processes of the Components involved in FLISR

Except for the actuators, the other cyber components involved in the FLISR process, namely sensors, CBCs, FOs, and SWs can be modeled using a two-state Markov process, because their failure can be immediately detected. They can then be easily incorporated into the SMCS. The failures of the actuators may not always be detectable. We assume that the failure of an actuator can be detected immediately after its failure with probability ρ_1, while a percentage of its failures can be detected with periodic inspections (type **I** hidden failure with probability ρ_2). Finally, a percentage of their failure cannot be detected unless their operation is required (type **II** hidden failure with probability ρ_3). Obviously, a type **I** hidden failure can also be detected if the operation of the related
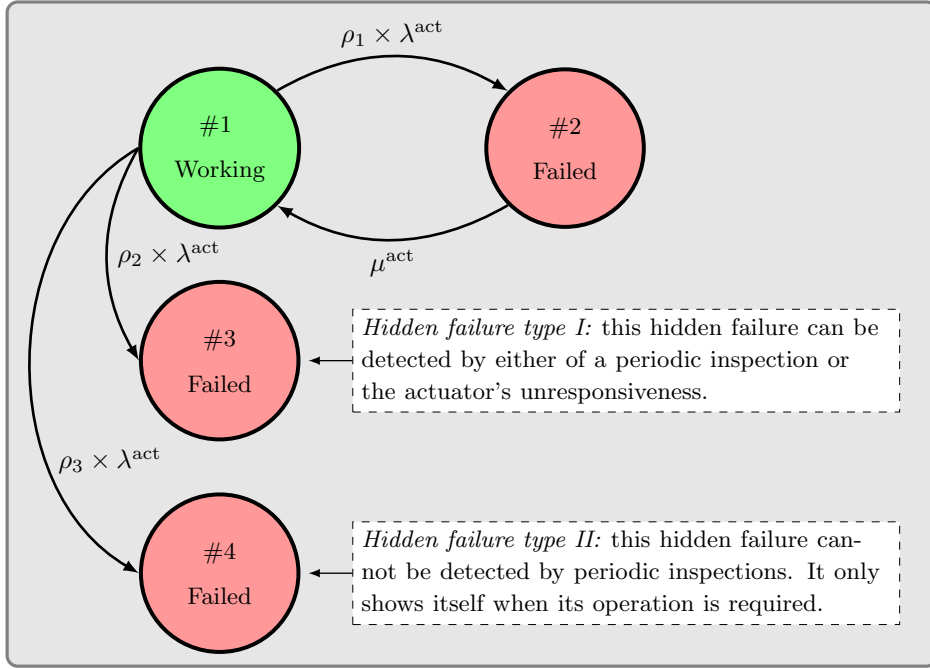
10

Figure 3: Markov model for the actuators of power switches.

actuator is required before the inspection and $\rho_1 + \rho_2 + \rho_3 = 1$. According to the explanation, an actuator with failure rate λ^{act} and repair rate μ^{act} can be represented by the Markov model depicted in Figure 3. The model itself is not complete since it requires the failure of power components and the addition of periodic inspections to exit states #3 and #4. The procedure for the incorporation of this model into SMCS is explained later. It is also worth mentioning that if there is no periodic inspection, states #3 and #4 are merged into one state.

2.4.5. Manual Switching

In cases where manual switching is available to 1) minimize the faulted area and 2) maximize service restoration, where some necessary cyber components have failed in the first place, two situations are probable:

1. The power switches that had to operate (execute open/close commands) to attain the aforementioned objectives are known, but they did not operate as a result of the failure of relevant actuators, cyber links, and/or CBCs. Let τ_1^{msw} be the probability density function for the manual switching time in this case. All the power switches whose operations are required for service restoration logically follow this manual switching time, since these power switches are determined by the central processor itself. The power switches involved in the fault isolation that did not operate because of the failure of their actuator are also in this category. Note that this describes a case in which automatic switching has already failed.

11

2. The switches whose operation can decrease the faulted area but are not exactly known by the central controller. Let τ_2^{msw} be the probability density function of manual switching time in this case. These are the power switches involved in fault location and isolation that cannot exchange information with the central processor. For manual switching in this case, the location of the fault should be first determined.

It is assumed that both manual switching times (τ_1^{msw} and τ_2^{msw}) follow log-normal distribution [30]. The average time for manual switching τ_1^{msw} is less than the average manual switching time τ_2^{msw} because in the first case, the power switches that should operate are already known.

2.4.6. Adjusting the Output of SMCS to Incorporate Manual Switching

In this study, we first generate a yearly sample using SMCS and then analyze it. The output of SMCS is adjusted as follows to incorporate manual switching. Assume a system state s_i starts at t_i. If manual switching is required in this state, it is first determined whether the manual switching follows the distribution τ_1^{msw} or τ_2^{msw}. A sample is then drawn from the related probability density function. Let the sample time be Δt. In this case, another state starting at $t_i + \Delta t$ is added and the open/close status of the switches in the added state is updated according to the manual switching. If the failure in the system that caused the inaccessibility of the target power switch is repaired sooner than sample ΔT, no adjustment is required.

2.4.7. Adjusting the Output of SMCS to Incorporate the Hidden Failures of Actuators

To adjust the output of SMCS to properly incorporate the presented Markov model of actuators into the simulation, the first step is to determine the schedule of the periodic inspections. Assume that a yearly inspection is carried out on the first day of April at t_i for an actuator. Having this information as a backdrop, if the actuator is in state #3 in the output of SMCS at this time period, it is changed to #2 at the beginning of this time period. In addition, any required operation of the actuator that reveals its type **I** and **II** hidden failures changes its state to #2. For both cases, a sample is drawn from state #2 based on its repair rate, and the yearly sample is amended accordingly.

2.4.8. Necessary Cyber Links for the Power Switches

The necessary cyber links for the operation of power switches differ depending on the design of the protection system used for fault clearing and on the design of the control system required for network reconfiguration. A local protection system requires proper operation of the power switch, and its local controller and measurement units, while differential protection of a zone requires proper operation of the power switches, and their controller and measurement units at both ends of the related zone together with the cyber link between the controllers. As discussed earlier, in a centralized protection system, the commands required for the operation of power switches are calculated and

Table 1: Types of Interdependencies and the Consequence of Cyber Failures Considered in this Study.

Failure	Impact	Consequence
DMS	Direct	Shifting of all MGs to the islanding mode
Cyber link between DMS and upstream grid	Direct	Disconnection of distribution network from upstream grid
MGCC	Direct	Shutdown of MG.
Cyber links between MGCC and DMS	Direct	Shift of the MG to islanding mode
All cyber links to/from MGCC	Direct	Shutdown of the MG
CBCs or all their necessary cyber links	Indirect	Inaccessibility of circuit breaker (mis-operation mode)
MCs or their connection to the corresponding MGCC	Direct	Outage of the corresponding DER
LCs or their connection to the corresponding MGCC	Indirect	Uncontrollable load point

sent by the central control system. In this study, it is assumed that the power switches inside an MG are solely controlled by their associated MGCC, and the power switches at POIs are controlled (for both protection and reconfiguration purposes) by either the neighboring MGCCs or the DMS, such that the DMS, $MGCC_1$, and $MGCC_2$ can provide the trip command for the power switch between the first and the second MGs in Figure 1. The availability of a cyber link between a power switch and any of its associated controllers results in its proper operation if the associated CBC and controller are working. Table 1 summarizes the interdependencies considered in this study.

2.5. Renewable Energy Resources, Loads, and Market Prices

To characterize the system behavior properly, due to the presence of ESS in the model, the temporal correlation of the renewable generation, loads, and market prices should be considered in the model. For simplicity, 19 years of historical data (2000–2018) on wind speed and solar irradiation, one year of historical data on market prices [23], and the IEEE-RTS load profile [23] are repeatedly used in this study. The historical data of wind speed and solar irradiation, obtained from [31], belong to Spain at latitude 36.8573 and longitude -2.5147. Note that hourly wind speed and solar irradiation have been transformed to power production according to the method explained in [23]. Two alternatives are feasible to comprehensively incorporate these sources of randomness into the analysis for a realistic case study. First, similar yearly historical data of market prices, solar irradiation, wind speed, and loads of an arbitrary number of years — the higher, the more accurate — can be considered if the data are available. Alternatively, a scenario generation method that takes the correlation among these random variables and their own temporal correlation into account can be applied but is beyond the scope of this paper.

3. System Operation

The operation mode of an MMG system might change due to the different contingencies in both cyber and power systems. Consequently, different operation modes are required to properly characterize the system behavior as follows:

i. *Normal Operation* (NO): The MGs connect to the upstream grid and can trade power both with the upstream grid and with each other.

ii. *Joint Operation* (JO): A number of MGs are connected to each other and can trade power among themselves but are separated from the upstream grid.

iii. *Islanding Operation* (IO): The islanded MG operates individually and is disconnected from the rest of the network.

iv. *Shutdown Mode* (SD): All load points are interrupted and all generation resources are disconnected from the MG.

In some situations, there may be different operation modes for different MGs in an MMG system; for example, some MGs may be in joint operation mode and others may be in islanding mode. This occurs, for example, due to a simultaneous failure in the upstream grid and one of the circuit breakers between the MGs in Figure 1. This case would result in the joint operation of two of the MGs and the islanding operation of the other one. In addition, with the presence of protection devices inside the MGs, a part of an MG might be separated (and shut down) while the rest might be in normal, joint, or island operation modes.

When a failure occurs that causes the separation of the distribution network from the upstream grid or causes the unintentional islanding operation of an MG, the lack of local generation resources causes load interruption. Therefore, it is essential to characterize these modes for acquiring the adequacy indices. In addition, to obtain an accurate result, it is necessary to simulate the normal operation of the system prior to the contingency. This is required to obtain the initial State of Charge (SOC) of the ESS and any other time dependent generation resources or loads at the beginning of the contingency [32]. For the last operation mode, namely shutdown mode, no scheduling strategy is required, and the ESSs maintain their states of charge. Following the aforementioned explanation, three mathematical problem formulations are defined as follows: **P1**: *Normal Operation* (NO), **P2**: *Islanding Operation* (IO), and **P3**: *Joint Operation* (JO).

This section separately formulates each of these problems. The main symbols used in this section are listed in Table 2.

3.1. Normal Operation Mode (P1)

MGCC–P1: In the NO mode, the objective of each MG is to minimize its operation cost, ξ_m^{GC}. The optimization problem for the daily scheduling of each MG ($m \in \mathcal{M}$) in NO mode is as follows:

Table 2: Notation and Symbols.

Superscripts	
de/w/pv	Diesel engine / Wind unit / PV unit.
ess/ch/dch	Energy storage system / Charging / Discharging.
ls/lp/mg	Load shedding / Load point / Microgrid.

Indices and Sets	
$\mathcal{D}_m(d)$	Set (index) of diesel engines in microgrid m.
$\mathcal{R}_m(r)$	Set (index) of load segments in microgrid m.
$\bar{\mathcal{R}}_l(\bar{r})$	Set (index) of load segments at load point l.
$\mathcal{T}(t)$	Set (index) of time.
$\mathcal{M}(m, n)$	Set (indices) of microgrids.
$\mathcal{M}_{mn}$	Set of microgrids that utilize line mn for power exchange.

Parameters	
$\underline{C}^{\text{ess}}, \bar{C}^{\text{ess}}$	Minimum and maximum allowable state of charge of ESS.
$\eta^{\text{ch}}, \eta^{\text{dch}}$	ESS charging/discharging efficiency.
$\bar{\mathcal{P}}^{\text{de}}$	Maximum power production of diesel engine.
$\bar{\mathcal{P}}^{\text{ch}}, \bar{\mathcal{P}}^{\text{dch}}$	Maximum charging and discharging rates.
λ^{ex}	Electricity price.
$\lambda^{\text{sell}}/\lambda^{\text{buy}}$	Price of sold/purchased energy.
$\lambda^{\text{ch}}/\lambda^{\text{dch}}$	Cost of charging/discharging of ESS.
λ^{de}	Cost of thermal units.
λ^{emi}	Emission cost of thermal units.
$\lambda^{\text{ls-mg}}$	Cost of load shedding.
$\bar{\mathcal{P}}^{\text{w}}$	Maximum available power of wind unit.
$\bar{\mathcal{P}}^{\text{pv}}$	Maximum available power of PV unit.
ϕ^{*}	Availability of component * (obtained by MCS).

Continuous Variables	
$\mathcal{P}^{\text{de}}$	Generated power of thermal unit.
$\mathcal{P}^{\text{ch}}$	Amount of charging power of ESS at the grid side.
$\mathcal{P}^{\text{dch}}$	Amount of discharging power of ESS at the grid side.
$\mathcal{P}^{\text{ex}}$	Exchange energy among microgrids.
$\mathcal{P}^{\text{buy}}/\mathcal{P}^{\text{sold}}$	Purchased/sold energy from/to the microgrids.
$\mathcal{P}^{\text{ls-mg}}$	Load shedding.
c^{ess}	State of charge (SOC) of ESS (actual energy in MWh).
$\mathcal{P}^{\text{sub}}$	Purchased/sold energy from/to the distribution network.

3.1.1. Objective Function

$$\xi_m^{\mathrm{GC}}(\gamma_{1m}) = \sum_{t \in T} \begin{bmatrix} \mathcal{P}_{mt}^{\mathrm{buy}} \cdot \lambda_t^{\mathrm{buy}} - \mathcal{P}_{mt}^{\mathrm{sell}} \cdot \lambda_t^{\mathrm{sell}} \\ +\mathcal{P}_{mt}^{\mathrm{ch}} \cdot \lambda_m^{\mathrm{ch}} + \mathcal{P}_{mt}^{\mathrm{ch}} \cdot \lambda_m^{\mathrm{dch}} \\ + \sum_{d \in \mathcal{D}_m} \left[(\lambda_{md}^{\mathrm{de}} + \lambda_{md}^{\mathrm{emi}}) \cdot \mathcal{P}_{mdt}^{\mathrm{de}} \right] \\ + \sum_{r \in \mathcal{R}_m} \lambda_{mrt}^{\mathrm{ls\text{-}mg}} \cdot \mathcal{P}_{mrt}^{\mathrm{ls\text{-}mg}} \end{bmatrix} \cdot \Delta_t, \tag{1}$$

where γ_{1m} is the set of decision variables for MG m. For simplicity, during normal operation, it is assumed that MGs are price takers, and there is no service (transmission) cost and losses, which results in the same purchase and sale prices. These assumptions are acceptable since normal operation is only required for obtaining the initial state of the ESSs at the beginning of a contingency. The first row in the objective function, according to the aforementioned assumptions, can be replaced by $\mathcal{P}^{\mathrm{ex}} \cdot \lambda_t^{\mathrm{ex}}$, where the sign of $\mathcal{P}^{\mathrm{ex}}$ is negative for sold energy and positive for purchased energy. Let $\xi_m^{\mathrm{GC}'}$ be the new objective function for later usage. The terms in the second row are the cost of charging and discharging of ESSs. The term in the third row is the cost of diesel engines, considering their fuel and emission costs. The fourth row yields the cost of load shedding in the MG. γ_{1m} is the set of decision variables for MG m. Note that in normal operation mode, the upstream grid fully supports the distribution network and there is no energy deficit. In this regard, there will be no interrupted load in this mode due to an energy deficit. The problem is subject to the constraints outlined below.

3.1.2. DER constraints

$$0 \leq \mathcal{P}_{mt}^{\mathrm{ch}} \leq \bar{\mathcal{P}}_m^{\mathrm{ch}} \cdot \phi_{mt}^{\mathrm{ess}} \qquad\qquad\qquad : \forall t \in \mathcal{T}, \tag{2}$$

$$0 \leq \mathcal{P}_{mt}^{\mathrm{dch}} \leq \bar{\mathcal{P}}_m^{\mathrm{dch}} \cdot \phi_{mt}^{\mathrm{ess}} \qquad\qquad\qquad : \forall t \in \mathcal{T}, \tag{3}$$

$$c_{mt}^{\mathrm{ess}} = c_{m,t-1}^{\mathrm{ess}} + \left(\mathcal{P}_{mt}^{\mathrm{ch}} \cdot \eta^{\mathrm{ch}} - \mathcal{P}_{mt}^{\mathrm{dch}} / \eta^{\mathrm{dch}} \right) \cdot \Delta_t \qquad : \forall t \in \mathcal{T}, \tag{4}$$

$$\underline{C}_m^{\mathrm{ess}} \leq c_{mt}^{\mathrm{ess}} \leq \bar{C}_m^{\mathrm{ess}} \qquad\qquad\qquad : \forall t \in \mathcal{T}, \tag{5}$$

$$c_{m,t_i}^{\mathrm{ess}} = c_{m,t_{end}}^{\mathrm{ess}}, \tag{6}$$

$$0 \leq \mathcal{P}_{mt}^{\mathrm{w}} \leq \bar{\mathcal{P}}_{mt}^{\mathrm{w}} \cdot \phi_{mt}^{\mathrm{w}} \qquad\qquad\qquad : \forall t \in \mathcal{T}, \tag{7}$$

$$0 \leq \mathcal{P}_{mt}^{\mathrm{pv}} \leq \bar{\mathcal{P}}_{mt}^{\mathrm{pv}} \cdot \phi_{mt}^{\mathrm{pv}} \qquad\qquad\qquad : \forall t \in \mathcal{T}, \tag{8}$$

$$0 \leq \mathcal{P}_{mdt}^{\mathrm{de}} \leq \bar{\mathcal{P}}_{md}^{\mathrm{de}} \cdot \phi_{mdt}^{\mathrm{de}} \qquad\qquad\qquad : \forall t \in \mathcal{T} \,\& \tag{9}$$

$$\forall d \in \mathcal{D}_m,$$

where (2) and (3) restrict the charging and discharging, respectively, of the ESS to their maximum amounts. Constraint (4) calculates the SOC of ESS. Constraint (5) limits the SOC of the ESS to its maximum and minimum allowable amounts. Constraint (6) states that the SOC of ESS at the end of scheduled horizon $c_{m,t_{end}}^{\text{ess}}$ should be equal to its initial amount c_{m,t_i}^{ess}. Note that the variable $c_{m,t}^{\text{ess}}$ is the actual energy of ESSs in MWh. The availability of the ESS, ϕ_{mt}^{ess}, is calculated as follows:

$$\phi_{mt}^{\text{ess}} = \phi_{mt}^{\text{ph-ess}} \cdot \phi_{mt}^{\text{mc-ess}} \cdot \phi_{mt}^{\text{cl-ess}}, \tag{10}$$

where the first, second, and third terms, on the right-hand side of (10) are the availability of physical ESS, its controller (MC), and the cyber link of its MC (obtained using MCS), respectively. Note that $\phi^* = 1$ yields that component * is working and $\phi^* = 0$ yields that components * has failed. Constraints (7) and (8) limit the power production of the wind and PV units, respectively, to their maximum available generation at each time period. Note that the randomness of these generation resources is considered in $\bar{\mathcal{P}}_{mt}^{\text{w}}$ and $\bar{\mathcal{P}}_{mt}^{\text{pv}}$. The availability of these units, ϕ_{mt}^{w} and ϕ_{mt}^{pv}, are calculated akin to the ESS availability, as in (10). Constraint (9) denotes the limitations of the diesel engine. The availability of these units, ϕ_{mdt}^{de}, are obtained akin to the ESS availability, as in (10).

3.1.3. Load Shedding Constraints

Due to the presence of load controllers, the loads at each load point can be interrupted partially based on their interruption (load shedding) costs. In this regard, each load point is defined as multiple segments indicating their priority. Let $\{\bar{\mathcal{R}}_l\}_{l \in \mathcal{L}} = \{\bar{r}|1,\ldots,N_{\bar{\mathcal{R}}_l}\}$ be a family of sets, where $\bar{\mathcal{R}}_l$ and $N_{\bar{\mathcal{R}}_l}$ are the set and number of load segments of load point l, respectively. Each segment is then represented by $(\theta_{l,\bar{r}}, \lambda_{l,\bar{r}}^{\text{ls-lp}})$, where $\theta_{l,\bar{r}}$ is the proportion of segment $\bar{r}$ w.r.t. the total demand of the load point l (L_l^{lp}), and $\lambda_{l,\bar{r}}^{\text{ls-lp}}$ indicates its associated load shedding cost. To provide a uniform load shedding of the load points in an MG, the load of the segments with the same load shedding cost is aggregated in one variable. Let $\{\mathcal{R}_m\}_{m \in \mathcal{M}} = \{r|1,\ldots,N_{\mathcal{R}_m}\}$ be a family of sets where $\mathcal{R}_m$ is the set of load segments of MG m. $N_{\mathcal{R}_m}$ is the number of unique interruption costs in the MG m. The load segment r in MG m is then associated with the interruption cost $\lambda_{m,r}^{\text{ls-mg}}$. Therefore, $\forall_r \in \mathcal{R}_m \,\& \,\forall_t \in \mathcal{T}$:

$$(1 - \phi_{lt}^{\text{tr}}) \cdot \sum_{l \in \mathcal{L}_m} \theta_{l,\bar{r}'} \cdot L_{l,t}^{\text{lp}} \leq \mathcal{P}_{mrt}^{\text{ls}} \leq \phi_{lt}^{\text{lc}} \cdot \sum_{l \in \mathcal{L}_m} \theta_{l,\bar{r}'} \cdot L_{l,t}^{\text{lp}}, \tag{11}$$

where, $\bar{r}'$ is equal to $\bar{r}$ such that $\lambda_{m,l,\bar{r}}^{\text{ls-lp}} = \lambda_{m,r}^{\text{ls-mg}}$. In other words, $\bar{r}'$ is the segment of load point l whose associated interruption cost is equal to the associated cost of segment r of the MG. ϕ_{lt}^{tr} is the availability of the transformer of load point l. ϕ_{lt}^{lc} is the availability of the load controller of load point l and is equal to the availability of the load controller itself times the availability of its associated cyber link. The load demand of segment r at MG m that should be supplied is then
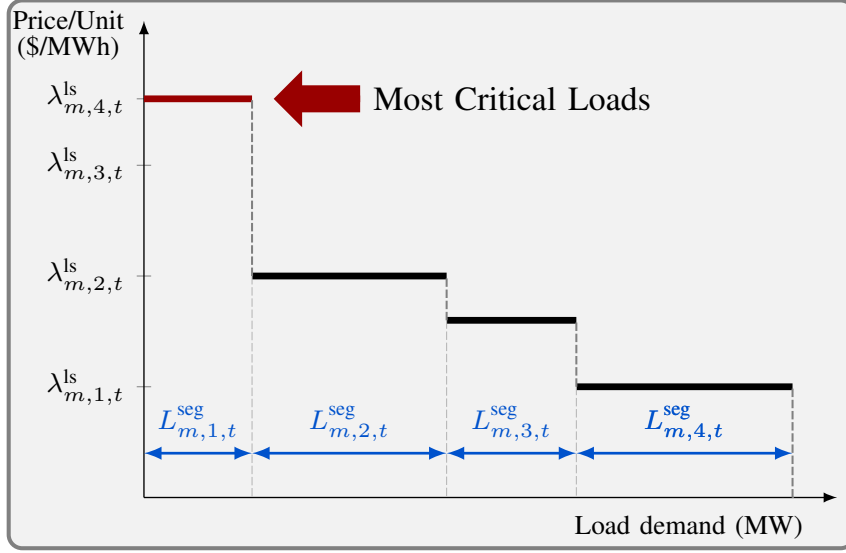
Figure 4: Illustration of four load segments.

$L^{\text{seg}}_{mrt} = \phi^{\text{tr}}_{lt} \cdot \sum_{l \in \mathcal{L}_m} \theta_{l,\bar{r}'} \cdot L^{\text{lp}}_{l,t}$. Figure 4 shows the aggregated load segments with their associated load shedding costs for an MG with four load segments.

3.1.4. Power Balance Constraints

$$\sum_{d \in \mathcal{D}_m} \mathcal{P}^{\text{de}}_{mdt} + \mathcal{P}^{\text{dch}}_{mt} - \mathcal{P}^{\text{ch}}_{mt} + \mathcal{P}^{\text{w}}_{mt} + \mathcal{P}^{\text{pv}}_{mt} + \mathcal{P}^{\text{ex}}_{mt}$$
$$= \sum_{r \in \mathcal{R}_m} L^{\text{seg}}_{mrt} - \sum_{r \in \mathcal{R}_m} \mathcal{P}^{\text{ls}}_{mrt} : \quad \forall t \in \mathcal{T}. \tag{12}$$

Overall, the following equations summarize the mathematical problem formulation of **MGCC– P1** during its normal operation:

$$\mathbf{MGCC - P1:} \quad \min_{\gamma_{1_m} \in \Gamma_{1_m}} \quad \xi^{\text{GC}'}_m(\gamma_{1_m}), \tag{13}$$

s.t.: (2) to (9), (11) and (12),

over: $\gamma_{1_m} = \begin{cases} \mathcal{P}^{\text{ex}}_{mt}, \mathcal{P}^{\text{w}}_{mt}, \mathcal{P}^{\text{pv}}_{mt} & : \forall t \in \mathcal{T} \\ \mathcal{P}^{\text{ch}}_{mt}, \mathcal{P}^{\text{dch}}_{mt}, c^{\text{ess}}_{mt} & : \forall t \in \mathcal{T} \\ \mathcal{P}^{\text{de}}_{mdt} & : \forall t \in \mathcal{T} \,\&\, \forall d \in \mathcal{D}_m \\ \mathcal{P}^{\text{ls-mg}}_{mrt} & : \forall t \in \mathcal{T} \,\&\, \forall r \in \mathcal{R}_m \end{cases}$.

DMS–P1: MGCCs solve the optimization problem **MGCC–P1**, and the resulting optimal value of purchased/sold power ($\mathcal{P}^{\text{ex}}_{mt} : \forall t \in \mathcal{T}$) is input to the DMS. Since the MGs are price takers, and a single price has been considered for each time interval in normal operation mode, there are no conflicts of interest between the MGs except when a line is congested. In this regard, the DMS

18

checks the feasibility of these power exchange values w.r.t. the capacity of the lines. The thermal capacity of a line is generally assumed to be rigid, and no overloading is permitted.

A directed graph $G = (\mathcal{M}, \mathcal{E})$ can represent a radial MMG system. Let $\mathcal{M} := \{1, ..., N_\mathcal{M}\}$ denote the collection of all nodes. Each line connects an ordered pair (m, n) of nodes, where node m is the sending end MG and node n is the receiving end MG. Let $\mathcal{E}$ denote the collection of all lines, and $(m, n) \in \mathcal{E}$ is abbreviated by $m \to n$ for convenience. Note that since G is directed, if $(m, n) \in \mathcal{E}$, then $(n, m) \notin \mathcal{E}$. For each $t \in \mathcal{T}$, solving (14) for all $m \in \mathcal{M}$ gives the exchanged power through the lines between the MGs, and (15) provides power exchange from/to the upstream grid.

$$\mathcal{P}^{\text{line}}_{mnt} = \mathcal{P}^{\text{ex}}_{nt} + \sum_{k:n \to k} \mathcal{P}^{\text{line}}_{nkt} \qquad : \forall_t \in \mathcal{T} \ \& \ \forall_{(m,n)} \in \mathcal{E}, \tag{14}$$

$$\mathcal{P}^{\text{sub}}_t = -\sum_{m \in \mathcal{M}} \mathcal{P}^{\text{ex}}_{mt} \qquad : \forall_t \in \mathcal{T}. \tag{15}$$

Thereafter, the DMS checks the power exchange of the lines for any violation of their limits, as follows:

$$-\bar{\mathcal{P}}^{\text{line}}_{mnt} \leq \mathcal{P}^{\text{line}}_{mnt} \leq \bar{\mathcal{P}}^{\text{line}}_{mnt} \qquad : \forall_t \in \mathcal{T} \ \& \ \forall_{(m,n)} \in \mathcal{E}, \tag{16}$$

$$-\bar{\mathcal{P}}^{\text{sub}}_t \leq \mathcal{P}^{\text{sub}}_t \leq \bar{\mathcal{P}}^{\text{sub}}_t \qquad : \forall_t \in \mathcal{T}. \tag{17}$$

Provided that there is no line limit violation, the DMS submits a confirmation signal to the MGCCs, and the power production of the MGs will be according to their submitted schedule. In the case that a line limit is violated, conflicts might occur between different MGs. This conflict can be illustrated briefly by a case whereby two MGs are aiming to sell power to the upstream grid using the same line, but the aggregated power is more than the line capacity. The question then is: *How to assign the line capacity to the MGs?* This study deals with this as a *bankruptcy problem* [32] that handles the division of insufficient resources between the claimants. Various division rules can be implemented based on this concept and the agreements between the MGs, namely equal shares, equal shares of deficits, and Proportional Shares (PS). Here, PS is used which mathematically, $\forall_t \in \mathcal{T}$, and the line $m \to n$ is implemented as in (18). Note that since line congestion might occur in both directions, $\alpha = \text{sgn}\left\{\sum_{m \in \mathcal{M}_{mn}} \mathcal{P}^{\text{ex}}_{mn}\right\}$ is defined to consider the direction of the power flow, where sgn is the sign function.

$$\text{PS:} \begin{cases} \psi = \dfrac{\sum_{m \in \mathcal{M}''_{mn}} |\mathcal{P}^{\text{ex}}_{mt}|}{\bar{\mathcal{P}}^{\text{line}}_{mn} + \sum_{m \in \mathcal{M}'_{mn}} |\mathcal{P}^{\text{ex}}_{mt}|}, & \tag{18a} \\[4ex] \mathcal{P}^{\text{ex}*}_{mt} = \mathcal{P}^{\text{ex}}_{mt} \cdot \psi & : \forall_m \in \mathcal{M}'_{mn}, \tag{18b} \end{cases}$$
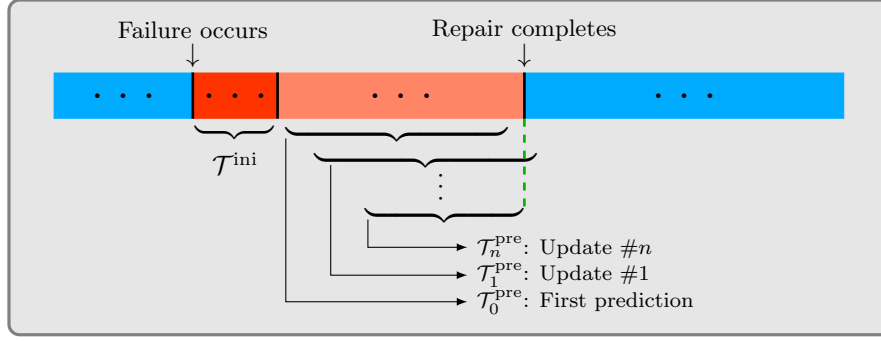
Figure 5: Graphic illustration of the different sets of time periods from the occurrence of a failure until its repair. $\mathcal{T}^{\mathrm{ini}}$: Set of time periods required for making the initial prediction of the time to repair. $\mathcal{T}_i^{\mathrm{pre}}$: Set of i-th prediction of repair time.

where $\mathcal{M}'_{mn} = \{m|m \in \mathcal{M}_{mn}, \alpha \cdot \mathcal{P}^{\mathrm{ex}}_{mt} \geq 0\}$, and $\mathcal{M}''_{mn}$ indicates its complement w.r.t. $\mathcal{M}_{mn}$. Solving (18a) gives ψ, which is then used to obtain $\mathcal{P}^{\mathrm{ex}^*}_{mt}$ using (18b). The DMS then submits $\mathcal{P}^{\mathrm{ex}^*}_{mt}$ to the MGCCs, whereby each MGCC solves **MGCC–P1** by considering a constraint for its power exchange $\mathcal{P}^{\mathrm{ex}}_{mt}$ with respect to $\mathcal{P}^{\mathrm{ex}^*}_{mt}$. This process is repeated until there is no violation in line capacities.

3.2. Uncertainty of the Contingency Duration

Due to the temporal correlation of ESSs, it is essential to have a strategy in place to deal with the uncertainty associated with time to repair. In this regard, a method is developed that uses the prediction of the contingency duration (that is updated during the contingency) to cope with this uncertainty. As shown in Figure 5, during a contingency and after the elapse of a certain number of time periods ($\mathcal{T}^{\mathrm{ini}}$), the first prediction of the remaining repair time ($\mathcal{T}_0^{\mathrm{pre}}$: first prediction) is assumed to be available. A prediction of the remaining time to repair should be provided to the model either by the system operator or with any other predefined logics in the controllers. This prediction can be updated in the course of the contingency. With each update i of the prediction ($\mathcal{T}_i^{\mathrm{pre}}$), a new optimization problem is solved for the remainder of the contingency. The initial SOC in this new optimization problem is obtained from the preceding optimization problem. Without loss of the generality of the proposed method, it is assumed that the first prediction is accurate for its application in this study. In this regard, two strategies, (A) and (B), are developed for island and joint operation modes for these two sets of time periods.

3.3. Island Operation Mode (P2)

MGCC–P2(A): First, an hourly conservative strategy is developed as follows for the operation of the islanded MG until a prediction for the duration of contingency is available.

$$\textbf{MGCC–P2(A):} \quad \min \left(\xi_m^{\mathrm{GC}\prime} \middle| \mathcal{P}^{\mathrm{ex}} = 0 \text{ and } T = t\right) + \lambda^{ess} * \left(c^{\mathrm{ess}}_{m,t-1} - c^{\mathrm{ess}}_{mt}\right) \qquad : \forall_t \in \mathcal{T}^{\mathrm{ini}} \quad (19)$$

20

$$\text{s.t.:} \qquad \text{(2) to (5), (7) to (9), (11) and (12),}$$

Since this problem is solved for only one time period, the ESSs will discharge their energy even if there is no load-shedding in the system. However, it is rational to possibly maintain the energy of ESSs or even charge them with cheaper energy for the upcoming time periods. In this regard, the term $\left(c^{\text{ess}}_{m,t-1} - c^{\text{ess}}_{mt}\right)$ with a positive multiplier λ^{ess} has been added to the objective function. By adding this term, an ESS will be charged if the marginal cost of the corresponding MG is lower than $\lambda^{\text{ess}} - \lambda^{\text{ch}}$ and will be discharged if the marginal cost of the system is higher than $\lambda^{\text{ess}} + \lambda^{\text{dch}}$. If, for example, it is desirable to charge the ESS with excess energy in the system and use the energy of ESS only for supplying loads with interruption cost higher than a specific value, different multipliers for charging and discharging powers should be used. By choosing λ^{ess} equal to the minimum interruption cost for a specific time period, this scheduling strategy decreases the load shedding at the highest possible level and only stores the excess energy in its ESS for upcoming hours. This may not be the best choice if the adequacy of the system is low.

Since the optimization problem **MGCC–P2(A)** is solved for one time period, an algorithm can be used to carry out the same task instead of the optimization problem. Such an algorithm is presented in the appendix.

MGCC–P2(B): After the first few time periods during a contingency when the prediction of repair time is available, the same optimization problem as **MGCC–P1** with $\mathcal{T} = \mathcal{T}^{\text{pre}}$ and $\mathcal{P}^{\text{ex}}_{mt} = 0$ is solved. In addition, constraint (6) is relaxed during the islanding operation. In this operation mode, only the signals regarding the status of the failure and the prediction of the repair time, if required, are exchanged between the MGCC and the DMS.

3.4. Joint Operation Mode (P3)

Unlike the islanding operation, the MGs in joint operation can exchange energy with each other. The MGs with different owners are self-interested: Each MG owner seeks its own operational and economic goals. This results in competition between the MGs for the power exchanges and the associated prices. On the one hand, the contingencies occur rarely and constitute a small proportion of the total system operation. On the other hand, this small proportion of time is the major cause of the loss of load in the system. Joint operation of the MGs occurs as a result of some of these contingencies. In this regard, to effectively supply the load demand, one option for the MGs is to cooperate with each other and coordinate their operation by sharing their on-site resources and flexible loads to prevent the interruption of critical loads based on predefined agreements. A fully coordinated operation, by forming a grand coalition, can be modeled by a single optimization problem with an objective equal to the sum of the objective functions of all MGs. There are several approaches for sharing the benefit of cooperative operation among the MGs using cooperative game theory solution concepts (such as the Shapley value, the Nucleolus, and equal sharing) [33]. However,

these are beyond the scope of this paper. In this study, a fully coordinated strategy for the joint operation of the MGs is considered that minimizes the overall load shedding cost. However, two new indices, explained in section 4.2, are proposed to calculate the impact of transactions on the interrupted loads in each of the MGs. The scheduling is carried out centrally by the EMS, and the dispatch orders are submitted to the MGCCs. The MGCCs then submit the necessary dispatch orders to their assets. In the same manner as section 3.3, and following the same logic, two strategies are developed for the mentioned sets of time periods during the joint operation mode.

P3(A): In the first couple of time periods $\mathcal{T}^{\mathrm{ini}}$, preceding the receipt of a prediction for the repair time $\mathcal{T}^{\mathrm{pre}}$, the system operation is carried out for one time period at a time.

The fully coordinated operation of the MGs during the joint operation, according to the aforementioned explanation, at time period t is obtained by the summation of (1) over $m \in \mathcal{M}^{\mathrm{jo}}$, as follows:

$$
\xi_t^{\mathrm{JO1}}(\gamma_{3(\mathrm{A})}) = \sum_{m \in \mathcal{M}^{\mathrm{jo}}} \begin{bmatrix} +\mathcal{P}_{mt}^{\mathrm{ch}} \cdot \lambda_t^{\mathrm{ch}} + \mathcal{P}_{mt}^{\mathrm{ch}} \cdot \lambda_t^{\mathrm{dch}} \\ + \sum_{d \in \mathcal{D}_m} (\lambda^{\mathrm{de}} + \lambda^{\mathrm{emi}}) \cdot \mathcal{P}_{mdt}^{\mathrm{de}} \\ + \sum_{r \in \mathcal{R}_m} \lambda_{mrt}^{\mathrm{ls}} \cdot \mathcal{P}_{mrt}^{\mathrm{ls}} \\ \lambda_t^{\mathrm{ser}} \cdot \mathcal{P}_{mt}^{\mathrm{buy}} \end{bmatrix} \cdot \Delta_t. \tag{20}
$$

Since this problem is solved for one time period, following the same logic explained in problem **MGCC–P2(A)**, the term $\left(c_{m,t-1}^{\mathrm{ess}} - c_{mt}^{\mathrm{ess}}\right)$ with a positive multiplier λ^{ess} should be added to the objective function. In addition, the assumption of neglecting service cost has been relaxed in **P–3(A)**, which results in the addition of the term in the last row in (20). This cost, which can represent either the transmission cost or the cost of energy loss, is required to prevent situations where an MG interrupts its load and sells it to another MG to supply its load with the same interruption cost. The problem is subjected to the following constraints:

$$(2) \text{ to } (5), (7) \text{ to } (9), (11), (12) \text{ and } (14) \text{ to } (17) \; : \forall_m \in \mathcal{M}^{\mathrm{jo}}.$$

P3(B): When the prediction for the repair time is available, the summation of the optimization problem (20) over $\mathcal{T} = \mathcal{T}^{\mathrm{pre}}$ is solved. The term $c_{mt}^{\mathrm{ess}} - c_{m,t-1}^{\mathrm{ess}}$ is not needed in this mode, as the system most likely shifts to grid-connected mode after $\mathcal{T}^{\mathrm{pre}}$. The objective function in this mode is then $\xi^{\mathrm{JO2}}(\gamma_{3(\mathrm{B})}) = \sum_{t \in \mathcal{T}^{\mathrm{pre}}} \xi_t^{\mathrm{JO1}}$. The EMS solves the following problem:

$$
\textbf{P3(B):} \quad \min_{\gamma_{3(\mathrm{B})} \in \Gamma_{3(\mathrm{B})}} \quad \xi^{\mathrm{JO2}}(\gamma_{3(\mathrm{B})}), \tag{21}
$$

s.t.: $\quad (2) \text{ to } (5), (7) \text{ to } (9), (11), (12) \text{ and } (14) \text{ to } (17) \; : \forall_m \in \mathcal{M}^{\mathrm{jo}}.$

4. Steps of the Simulation

A self-explanatory flowchart illustrating the overall steps of the proposed framework for calculating the adequacy indices, including MCS steps, is given in Figure 6.

4.1. Simulating Individual Components

To simulate the random behavior of the system, the failure and repair of the components are simulated through stochastic processes in MCS-based methods. In this study, the time to repairs and the time to failures were assumed to follow exponential distributions [34], which can be expressed as follows:

$$f(x) = \zeta e^{-\zeta x}. \tag{22}$$

Therefore, the time to the next event can be sampled using the following random variate:

$$X = -\frac{\ln(U)}{\zeta}, \tag{23}$$

where U is a uniformly distributed random number over $[0, 1]$. In (23), with respect to the state—in-service and out-of-service—of the component, failure rate or repair rate is used in place of ζ, respectively. Equation (23) is used repeatedly to sample up and down times (X) for each component during the entire simulation period. Note that the SMCS method used in this study for sampling the states of the whole system is known as "*state duration sampling*", as described in [34].

4.2. Adequacy Indices

This study calculates the well-known adequacy index, Expected Energy Not Supplied (EENS). However, other well-known adequacy indices for distribution networks can be easily calculated. In this study, the EENS index pertains to the actual interrupted load, which for segment r in MG m at hour t (of one hour resolution) of sample year y is equal to $\mathcal{P}_{mrt}^{\text{ls-mg}}$ obtained from the above problem formulations. The presence of load controllers in the smart grids enables an MG operator (or a load agent in multi-party MGs) to partly interrupt the loads with lower interruption cost and sell energy to the other MGs to prevent the interruption of loads with higher interruption cost. Although this will increase the value of the conventional adequacy index EENS for the seller MG, since this MG will be paid at least equal to the interruption cost of curtailed load, this load interruption is even beneficial for the MG. In addition, in some situations, a buyer MG supplies part of its load with an expensive energy resource. These are important for the system design and should be calculated to give the MGs a better basis for their investments and system design. To this end, two indices—IbGC & SbER—are proposed. The IbGC index represents the load demands that are Interrupted But Gained Compensation (IbGC). The SbER index represents the load demands that are Supplied By Expensive Resources (SbER). These indices are calculated based on the following rules:

Algorithm 1: Calculate IbGC and SbER.

Input : $\mathcal{P}_{mt}^{\text{buy}}, \mathcal{P}_{mt}^{\text{sell}}, \mathcal{P}_{mrt}^{\text{ls}}$: obtained from P3(A) and P3(B) and λ^{thr}.

Output: IbGC and SbER.

1 **for** $t \in \mathcal{T} = \{t \mid system\ is\ in\ joint\ operation\}$ **do**
2   **for** $m \in \mathcal{M}^{\text{sell}}$ **do**
3   **if** $\sum_{r \in \mathcal{R}_m} \mathcal{P}_{mrt}^{\text{ls}} \geq 0$ **then**
4          $d_1 = \mathcal{P}_m^{\text{sell}}$;
5   **for** $r \leftarrow N_{\mathcal{R}_m}$ **to** 1 **step** -1 **do**
6             $\text{IbGC}_{mrt} \leftarrow \min\left(\mathcal{P}_{mrt}^{\text{ls}}, d_1\right)$;
7             $d_1 = d_1 - \text{IbGC}_{mrt}$;
8   **end**
9   **end**
10   **end**
11   **if** $\sum_{m \in \mathcal{M}^{\text{sell}}} \sum_{r \in \mathcal{R}_m \mid \lambda_{mr}^{\text{ls}} \geq \lambda^{\text{thr}}} \mathcal{P}_{mrt}^{\text{ls}} \geq 0$ **then**
12   **for** $m \in \mathcal{M}^{\text{buy}}$ **do**
13          $d_2 \leftarrow \mathcal{P}^{\text{buy}}$;
14   **for** $k \leftarrow 1$ **to** $N_{\mathcal{R}_m}$ **step** $+1$ **do**
15             $\text{SbER}_{mkt} \leftarrow \min\left(L_{mrt}^{\text{seg}} - \mathcal{P}_{mkt}^{\text{ls}}, d_2\right)$;
16             $d_2 \leftarrow d_2 - \text{SbER}_{mkt}$;
17   **end**
18   **end**
19   **end**
20 **end**
21 $\mathcal{M}^{\text{sell}}$ and $\mathcal{M}^{\text{buy}}$ are the sets of seller and buyer MGs.
22 d_1 and d_2 are auxiliary variables.
23 $N_{\mathcal{R}_m}$ is the number of load segments in MG m.

- If an MG interrupts its load and sells energy simultaneously, it should gain compensation at least equal to the load's interruption cost.

- If the seller MG have interrupted loads with interruption cost higher than a predefined threshold λ^{thr}, the exchanged energy is considered to be expensive.

Mathematically, after solving the problem formulations **P3(A)** and **P3(B)**, these indices are calculated as per Algorithm 1.

5. Simulation Results

5.1. Input Data and the Simulation Software

Feeder 4 at bus 6 of Roy Billinton Test System (RBTS) [35] has been extended to form a CPMMG by adding DERs and the cyber infrastructure, as shown in Figure 7. The characteristics of the DERs are shown in Table 3. Types and interruption costs of the load points have been indicated in Table 4. These interruption costs were considered based on [36], where industrial loads type1 are agricultural sectors. The mean time to failure and repair of DERs are 5000 and 10 hours, respectively. The mean time to failure and repair of actuators and sensors are 87600 and 20 hours, respectively. The mean time to failure and repair of the upstream network is 15000 and 26 hours, respectively. The related
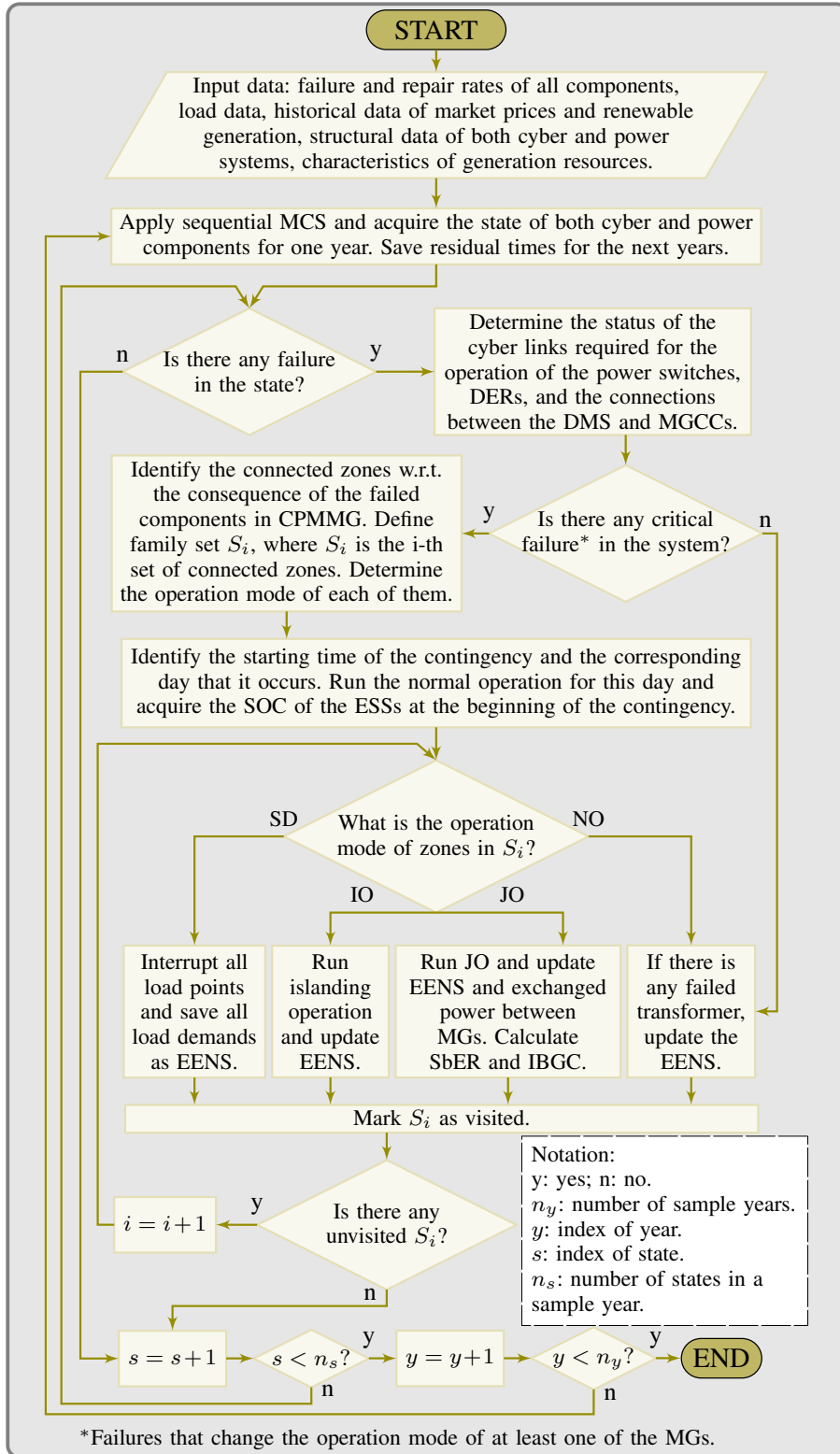
START

Input data: failure and repair rates of all components, load data, historical data of market prices and renewable generation, structural data of both cyber and power systems, characteristics of generation resources.

Apply sequential MCS and acquire the state of both cyber and power components for one year. Save residual times for the next years.

Is there any failure in the state? n / y

Determine the status of the cyber links required for the operation of the power switches, DERs, and the connections between the DMS and MGCCs.

Is there any critical failure* in the system? y / n

Identify the connected zones w.r.t. the consequence of the failed components in CPMMG. Define family set S_i, where S_i is the i-th set of connected zones. Determine the operation mode of each of them.

Identify the starting time of the contingency and the corresponding day that it occurs. Run the normal operation for this day and acquire the SOC of the ESSs at the beginning of the contingency.

What is the operation mode of zones in S_i? SD / IO / JO / NO

Interrupt all load points and save all load demands as EENS.

Run islanding operation and update EENS.

Run JO and update EENS and exchanged power between MGs. Calculate SbER and IBGC.

If there is any failed transformer, update the EENS.

Mark S_i as visited.

Is there any unvisited S_i? y → $i = i+1$ / n

$s = s+1$

$s < n_s$? y / n

$y = y+1$

$y < n_y$? y → END / n

Notation:
y: yes; n: no.
n_y: number of sample years.
y: index of year.
s: index of state.
n_s: number of states in a sample year.

*Failures that change the operation mode of at least one of the MGs.

Figure 6: Overall flowchart for calculating adequacy indices for CPMMG.

25

Table 3: Capacity of Distributed Generation in Each of the MGs.

Parameter	Unit	#	MG #1	MG #2	MG #3	MG #4	MG #5
$\bar{P}^{\mathrm{w}}$	(MW)	—	0.5	1.1	0.5	1	0.6
$\bar{P}^{\mathrm{pv}}$	(MW)	—	1.2	0.5	0.4	0.6	1
$\bar{P}^{\mathrm{ch}}$, $\bar{P}^{\mathrm{dch}}$	(MW)	—	0.4	0.3	0.2	0.25	0.4
η^{ch}, η^{ch}	—	—	0.98	0.98	0.98	0.98	0.98
$\bar{C}^{\mathrm{ess}}$	(MWh)	—	0.2	0.1	0.1	0.1	0.15
$\underline{C}^{\mathrm{ess}}$	(MWh)	—	1.2	0.8	0.5	0.8	1
$\bar{P}^{\mathrm{de}}$	(MW)	1	0.4	0.3	0.3	0.5	0.4
		2	0.3	0.5	—	0.5	0.4

Table 4: Interruption Costs of Different Sectors. Unit of Cost: $/MWh.

Sector & Type		Load priorities						Buses
		#1		#2		#3		
		%	cost	%	cost	%	cost	
Industrial	Type1	30%	0.1	70%	0.12	—	—	3,9,13,17,20,23
	Type2	15%	0.2	10%	2	75%	15.1	4,7,15,18,21
Commercial	—	20%	2	80%	12.87	—	—	2,8,12,16,22
Residential	—	30%	0.1	50%	0.15	20%	0.2	1,5,6,10,11,14,19

failure and repair rates of the rest of the components can be found in [23] except for the DMS, MGCC, and SW whose mean times to repair are reduced to 16 hours. The mean and standard deviation for τ_1^{sw} are 1.4 and 0.2, and for τ_1^{sw} are 1.6 and 0.4, respectively. ρ_1, ρ_2, and ρ_3—parameters of the Markov model of actuator—are 0.4, 0.3, and 0.3, respectively. Note that all the simulations were conducted in MATLAB® 2022a. It is also worth mentioning that the MCS method incorporates an error. Consequently, to ensure a fair comparison, the same set of samples obtained by SMCS (system states) was utilized in all case studies, except for the components whose failure and repair rates changed.

5.2. Impact of Cyber Failures in Various Operation Modes

Table 5 shows the EENS index for both case studies with ideal and non-ideal cyber systems for different load segments. For a more detailed analysis, we have separated the share of each operation mode in EENS for both case studies with ideal and non-ideal cyber systems. As an example, the shutdown mode in a case with the ideal cyber system occurs solely due to the failure of the distribution lines in that MG, while the shutdown mode in the case with the non-ideal cyber system also occurs as a result of the control system and FLISR malfunctioning. Note that shutdown modes also include partial shutdowns, where a part of an MG is down while the rest of it is operating in normal, joint, or islanding mode.

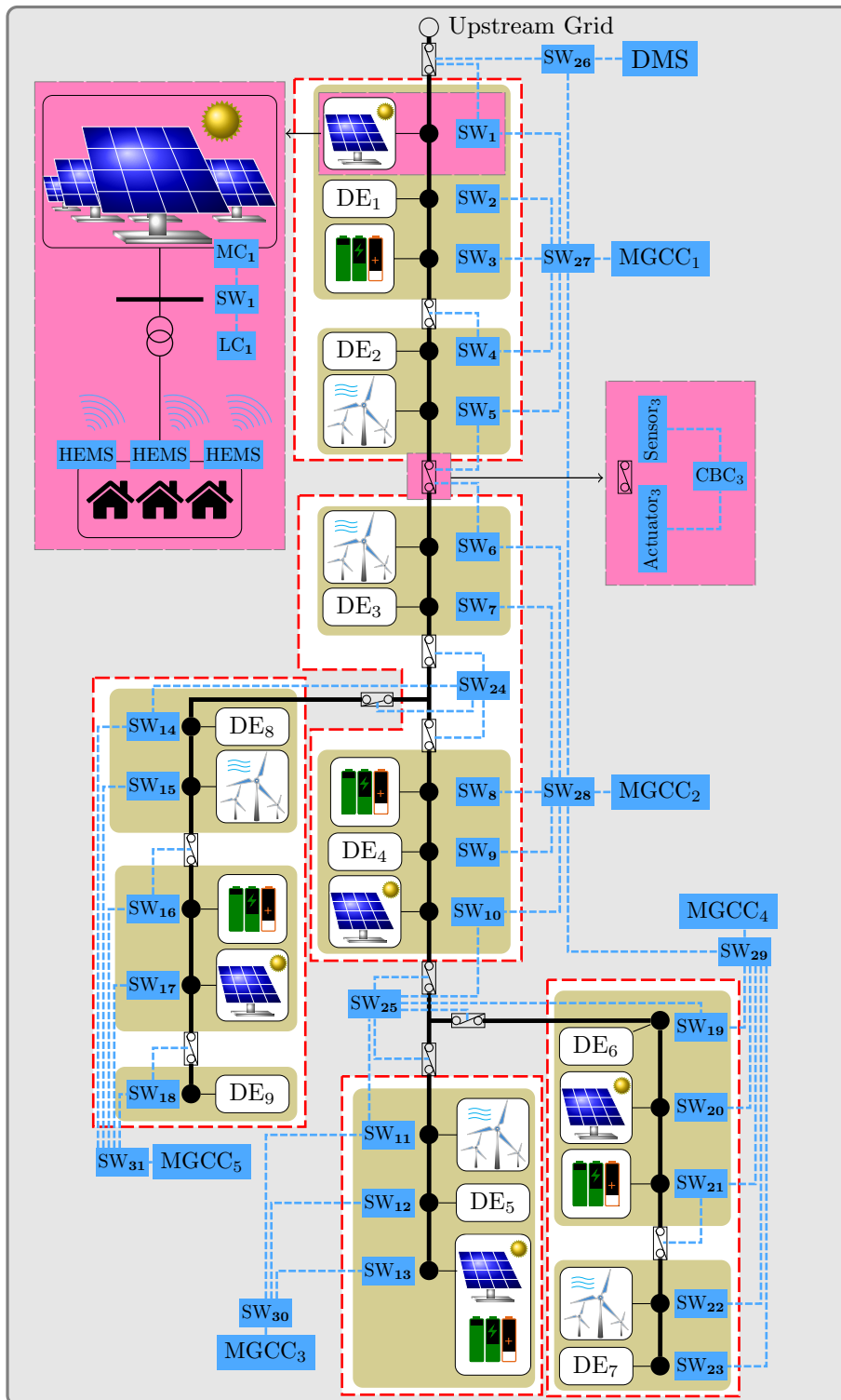The failures in the cyber system affect the EENS index in different operation modes; in this

Figure 7: Schematic diagram of the CPMMG under study. Tag number of the distribution buses are the same as the tag number of the network switches.

study, the shutdown and island modes are influenced the most. For shutdown mode, this is due, mostly, to the failure of the MGCC. The reason is that a centralized control system is responsible for the operation of the MGs, and its failure results in shutdown mode. For the island mode, this is due to the failure of the centralized DMS—whose failure shifts all MGs to island mode. It is concluded that the DMS and MGCCs are the most critical cyber components influencing the adequacy of a CPMMG. Consequently, to decrease the overall impact of cyber component failures on the adequacy of a CPMMG, it is crucial to deal with their failure. Two options are viable for handling this issue: 1) adding backup controllers for both DMS & MGCCs and 2) employing a distributed control system (or a control system that can shift to distributed control when required). These two options are further discussed in section 5.5. Similarly, the failure of each of the components in the cyber system can be analyzed w.r.t. the consequence of its failure.

Regardless of an ideal or non-ideal cyber system, other interesting observations can be made. First, in the presence of load controllers and DERs in the system, a proper strategy can efficiently decrease the interruption of the loads with higher interruption costs, which substantially reduces the total interruption cost. Second, through proper design of the system w.r.t. the location and the capacity of the DERs, the expensive loads are only interrupted during the normal and shutdown modes. In addition, during island mode in MG #5, load interruption slightly occurs in segments 5–7, as can be seen in Table 5. The reason is the islanding mode of the mid-section in this MG since there is no dispatchable DER in this zone.

Figure 8.a presents the convergence of the method w.r.t. the number of sample years for both ideal and non-ideal cyber systems. In addition, instead of the expected values, shown in Table 5, it is possible to derive the frequency of the yearly interrupted loads, as depicted in Figure 8.b and Figure 8.c, and consequently the distribution of yearly interrupted loads, which is beneficial for further analysis.

5.3. Internal Protection & Backup Supply

With respect to the failure rates considered in this study, except for the upstream grid, the distribution lines are the most influential factor for load interruption. Therefore, employing more power switches enhances the adequacy indices. The following cases are considered to study the impact of the presence of protection systems inside the MGs and a backup supply. Note that the backup supply is connected to bus #23 in Figure 7 by a normally open tie switch. The length of the adjacent feeder connected to the tie switch is assumed to be 15 km. Its failure rate is then 15 times the failure rate of the distribution lines. Its cyber link is assumed to be available if at least one communication route between this switch and either DMS or MGCC$_4$ is available. In this section, the failure of the upstream is omitted for a fair comparison. In addition, it is assumed that the distribution network can maintain its normal operation even when it loses its communication
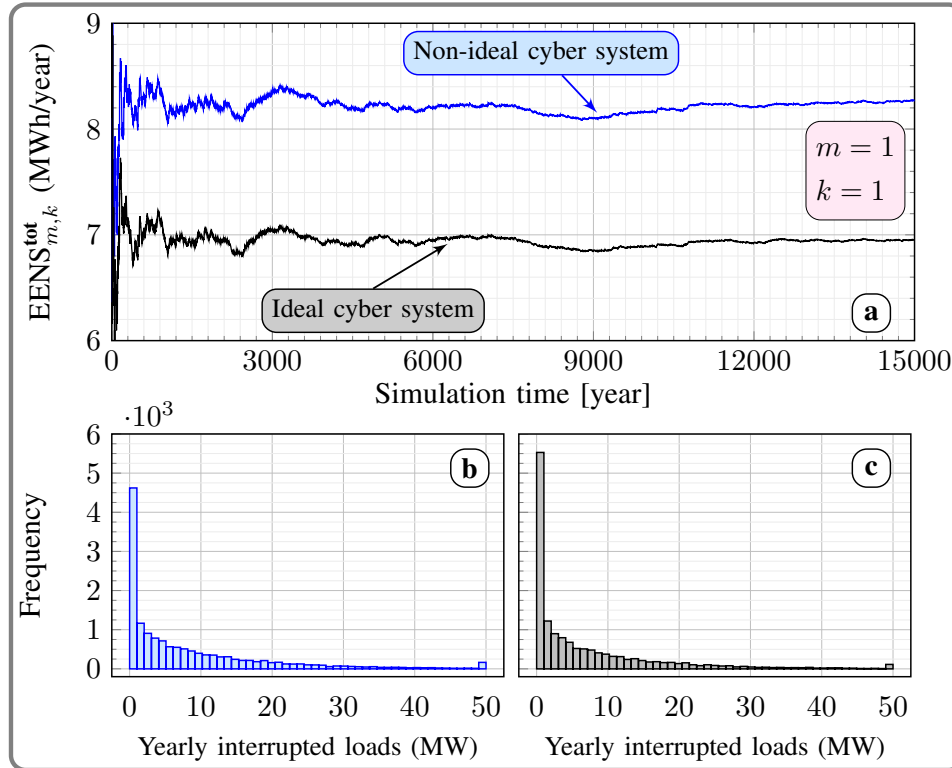
28

Figure 8: Convergence of the approach by increasing the simulation time.

channel to the upstream network.

- **Case I:** Only internal protection (more power switches)
- **Case II:** Neither internal protection nor backup supply
- **Case III:** Both internal protection and backup supply

Each of the above cases is further divided into three more cases, namely **a**, **b**, and **c**, with the following characteristics:

(a) Non-ideal cyber system, cyber topology as shown in Figure 7,

(b) Ideal cyber system,

(c) Non-ideal cyber system, cyber system includes spare controllers for the DMS and MGCCs with ring topology both among the MGCCs and inside MGs, as shown in Figure 10.

Figure 9 depicts the total EENS for cases I–III for all MGs. The results indicate that both internal protection and backup supply can improve the adequacy of the entire system. The internal protection, as shown in Figure 7, solely improves the system's adequacy by about 26%, and together with a backup supply connected to MG #4 improves the system's adequacy by 55%. Among the MGs, the least improvement, in the presence of only internal protection, takes place in MG #3 because MG #3 does not include internal protection. In addition, MGs #3 and #4 reap major benefits from the backup supply (about 60%) since they are closer to it.

Table 5: EENS During Different Modes of Operation for Ideal and Non-ideal Cyber Systems.

| MG tag | Segments | Contribution of each operation mode to EENS (MWh/year) | | | | | | | |
| | | Non-ideal cyber system | | | | Ideal cyber system | | | |
		JO	SD	IO	NO	JO	SD	IO	NO
MG #1	1	5.81	1.90	0.49	0.07	5.52	1.37	0.00	0.06
	2	4.90	1.46	0.37	0.05	4.66	1.01	0.00	0.04
	3	4.73	2.77	0.40	0.12	4.48	2.02	0.00	0.11
	4	0.20	0.59	0.03	0.02	0.19	0.41	0.00	0.02
	5	0.03	0.59	0.00	0.02	0.02	0.41	0.00	0.02
	6	0.00	1.35	0.00	0.03	0.00	1.00	0.00	0.03
	7	0.00	1.92	0.00	0.10	0.00	1.22	0.00	0.10
MG #2	1	9.63	3.44	0.46	0.06	8.85	2.92	0.00	0.05
	2	6.20	2.13	0.30	0.03	5.68	1.74	0.00	0.03
	3	8.54	5.64	0.44	0.11	7.83	4.81	0.00	0.10
	4	0.21	0.85	0.01	0.01	0.19	0.70	0.00	0.01
	5	0.02	0.94	0.00	0.02	0.01	0.76	0.00	0.02
	6	0.00	2.17	0.00	0.03	0.00	1.88	0.00	0.03
	7	0.00	3.01	0.00	0.09	0.00	2.20	0.00	0.09
MG #3	1	9.71	2.07	0.48	0.03	8.84	1.70	0.09	0.02
	2	4.41	1.03	0.21	0.02	4.02	0.85	0.04	0.02
	3	7.83	3.40	0.38	0.04	7.13	2.78	0.07	0.03
	4	0.06	0.41	0.00	0.01	0.06	0.34	0.00	0.01
	5	0.01	0.42	0.00	0.01	0.00	0.35	0.00	0.01
	6	0.01	1.69	0.00	0.02	0.00	1.38	0.00	0.02
MG #4	1	16.24	2.90	1.87	0.10	14.80	2.28	1.25	0.08
	2	4.38	1.08	0.21	0.01	3.99	0.91	0.04	0.01
	3	15.78	6.12	0.72	0.20	14.39	4.78	0.15	0.18
	4	0.06	0.43	0.00	0.00	0.06	0.36	0.00	0.00
	5	0.01	0.83	0.00	0.02	0.01	0.66	0.00	0.01
	6	0.00	1.02	0.00	0.02	0.00	0.72	0.00	0.02
	7	0.01	4.32	0.00	0.08	0.00	3.61	0.00	0.07
MG #5	1	7.03	1.54	1.86	0.05	6.51	1.21	1.13	0.03
	2	3.27	0.87	0.40	0.02	3.03	0.71	0.04	0.01
	3	11.52	3.09	2.19	0.10	10.67	2.34	0.87	0.07
	4	0.12	0.35	0.08	0.01	0.11	0.28	0.01	0.00
	5	0.05	0.77	0.18	0.02	0.04	0.56	0.04	0.02
	6	0.00	1.18	0.05	0.04	0.00	0.91	0.01	0.03
	7	0.00	3.56	0.00	0.08	0.00	2.50	0.00	0.08

The increase in the EENS due to failure of the cyber system when there is neither internal protection nor backup supply is 16%, while this value increases to 20% and 28% when adding only the internal protection and both the internal protection and backup supply, respectively. This is due, mostly, to the fact that the power system design has improved by adding additional options while the cyber system remained unchanged, and, therefore, its contribution to the total EENS increases.
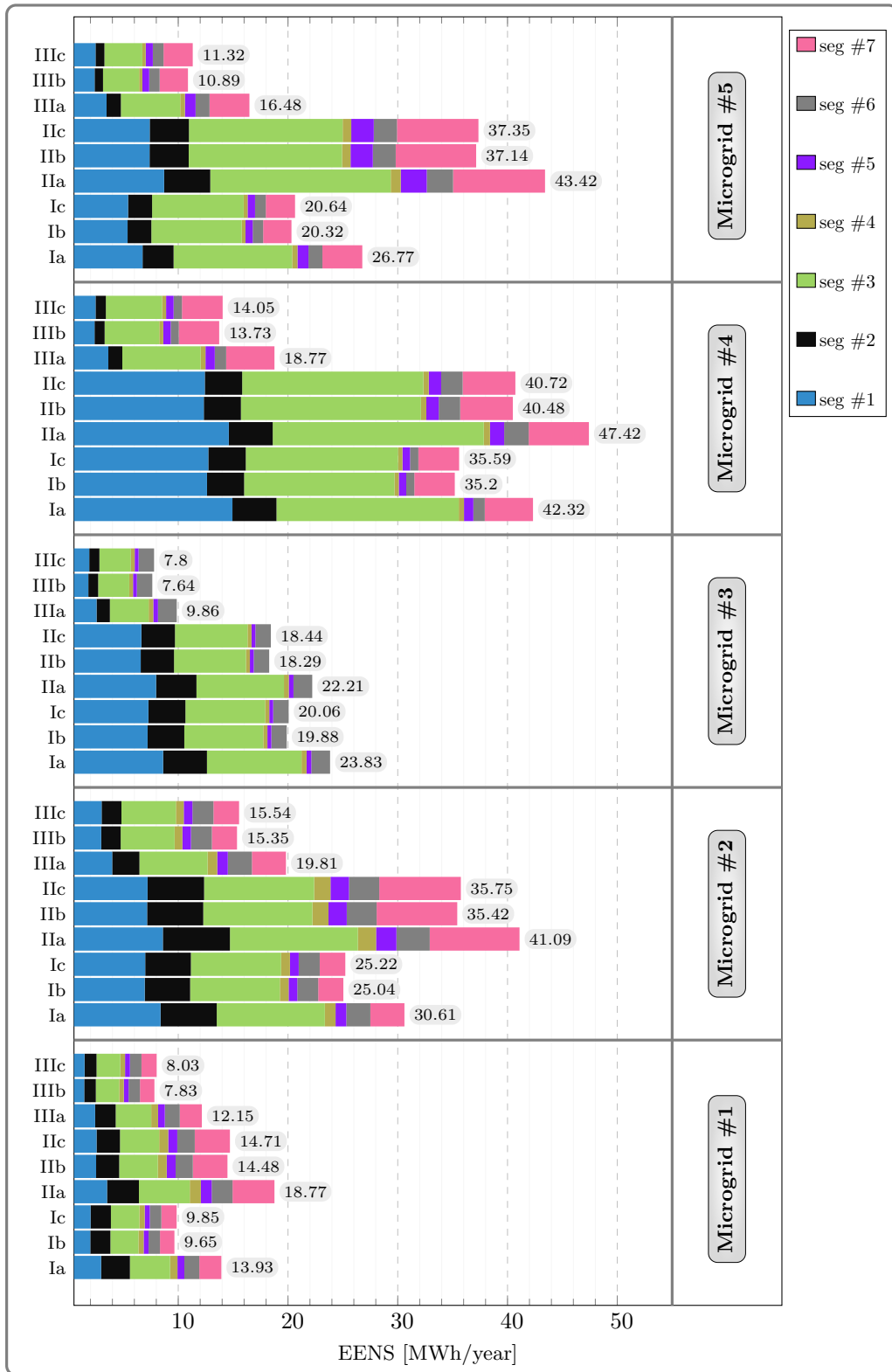
Figure 9: Impact of internal protection and backup supply on the overall EENS with and without the impact of cyber failures.
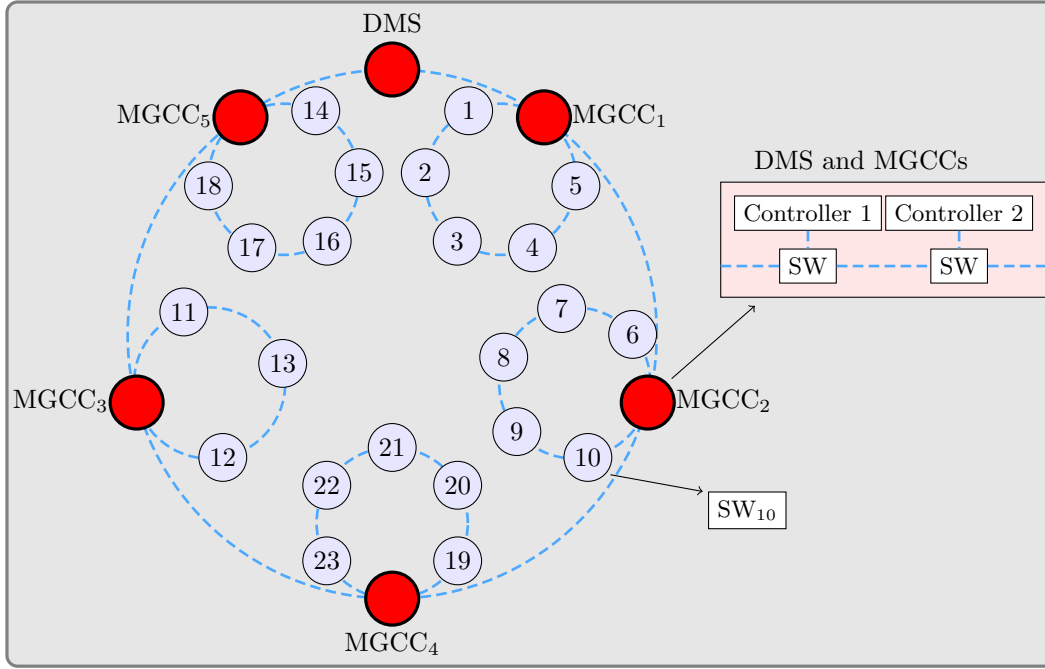
Figure 10: Cyber network topology: ring topology among MGCCs and the DMS, ring topology insider MGs, and spare controllers for both DMS and MGCCs.

5.4. Critical Cyber Components

As discussed, the failure of the main controllers (i.e., DMS, and MGCCs) has a high impact on the system adequacy. In the following, two options to deal with the failure of these components are discussed.

5.4.1. Spare Controller for the DMS and MGCCs

In this section, by adding spare controllers to the DMS and MGCCs, the impact of their failure is investigated. For this purpose, the topology shown in Figure 10 is implemented for the cyber network. The results are shown in Figure 9, in which the cases that end with **c** belong to this network topology. By comparing cases **(a)** and **(c)**, it is obvious that the failure of the DMS and MGCCs has a high impact on the adequacy of CPMMGs. In addition, by comparing cases **I(b)** and **I(c)**, the impact of the failure of the ICTs is only 1.15% higher than a case with an ideal cyber system. This value is further discussed in section 5.5.1.

5.4.2. Shift to Distributed Control System During Failure Events

The main drawback associated with a centralized control system is that the system is exposed to a single-point failure [37]; therefore, the system's adequacy mainly relies on the communication

system that is utilized. Using the proposed method, it is viable to derive a good approximation of the upper boundary of the adequacy indices for a distributed control system (or a system that can shift to the distributed control system when required). In this regard, when the DMS controller fails but all MGCCs are working, we can assume that the MGCCs can carry out the operation of the MMG system together in a distributed manner. In addition, when an MGCC fails but all MCs and LCs inside the related MG are working, we can assume that the MCs and LCs are able to carry out the operation of the related MG together in a distributed manner. This gives an upper boundary for the adequacy indices because a distributed control is assumed to be non-functioning with the simultaneous failure of controllers. However, the occurrence probability of such a case is very small. In this way, neglecting the failure of the main controllers—while the other necessary controllers required for a distributed control system are available—results in the upper boundary of the adequacy indices for a distributed control system. In this case, the adequacy index EENS is 1.24% higher than a case with an ideal cyber system. Comparing this value with 1.15% obtained in the previous section shows that the distributed control system can achieve almost the same result as a centralized control scheme with spare controllers. Although the failure and repair rates of ICT components require further research, the significant impact of the failure of these controllers on the adequacy of CPMMGs is clear. Therefore, the adoption of preventive actions, such as the ones explained here, seems to be necessary. Note that for the distributed control scheme, the interrupted loads were calculated using the scheduling strategies proposed for the centralized scheme. This is not a problem. With the improvements in the algorithms for distributed implementation of control systems, such a system is achievable.

5.5. Indirect Impacts

5.5.1. Power Switches in Mis-operation

The indirect impact of cyber component failures on FLISR is discussed in this section. First, to quantify this indirect impact, this impact is completely neglected in the simulation. The reference case in this section is **I(c)**. The total EENS of the system decreased by about 0.94%. This is almost equal to the difference between cases **I(b)** and **I(c)**. This means that by considering spare controllers for the DMS and MGCCs, what really diminishes the CPMMG adequacy—among cyber components—is the failure of components involved in FLISR processes. A question remains: which cyber components have the most impact in this case? To answer this question, two cases are simulated with the following characteristics:

1. There is no hidden failure in actuators, and all the failures of these components can be detected immediately ($\rho_1 = 1$ and ρ_2, $\rho_3 = 0$).
2. There are hidden failures in actuators, and no inspection is carried out ($\rho_1 = 0.4$, $\rho_2 = 0$, and $\rho_3 = 0.6$).

In the first case, the EENS index decreased by about 0.49%. Comparing this value with the reported value in the previous paragraph shows that hidden failures of the actuators are responsible for about 98% of the impact of the FLISR malfunction on the system's adequacy. The second case, in which the inspections were neglected, experienced a 0.41% increase in EENS, which shows the impact of a yearly inspection of the actuators on the adequacy indices. As the final point on the FLISR, note that the hidden failures of actuators exist in any scheme for the protection system; therefore, it can be concluded that a centralized scheme for FLISR is very little affected by cyber components failure.

5.5.2. Inaccessible Load Points

In this section, the indirect impact of inaccessible load points was calculated by neglecting them in the simulation results. Comparing this case with the base case shows almost no impact on the overall results. Generally, the impact of the failure of cyber components that have an indirect impact on the overall adequacy of a CPMMG is very low. The reason for this is that at least a simultaneous failure of a cyber component and a critical power component is required, whose probability of occurrence is very low.

5.6. Impact of scheduling Strategies

In this section, only the impact of one factor, i.e., the duration of initial hours $\mathcal{T}^{\text{ini}}$ on the adequacy of the system, is investigated. By increasing the number of time periods required for receiving a prediction of the duration of the contingency considered for the base case (one hour) to five hours, the total EENS of the whole system increases by less than 0.9%, which shows the effectiveness of the conservative strategy. However, this is less than the error of the MCS method and cannot be evaluated accurately except with an extremely large number of sample years.

5.7. Study of Proposed Indices—IbGC & SbER

For a coherent explanation of the proposed indices, some changes are made in the capacity of DERs and load types by including the MGs with the following properties: an MG that does not include industrial and commercial (expensive) loads but includes both dispatchable and non-dispatchable DERs (MG #1), and MGs with expensive industrial loads that do not include any dispatchable DERs (MGs #2 and #5). In addition, the capacity of the non-dispatchable DERs in MGs #1 and #2 is cut down to half of their capacity compared to the base case. The result for this case, as seen in Table 6, indicates that MG #1, as an MG that only includes residential and agricultural sectors, sells energy to the other MGs with expensive loads; therefore, the index IbGC for this MG is high in several load segments, while it does not supply any of its loads by expensive resources; this is reflected through the SbER index. Accordingly, MGs #2 and #5, with the absence of dispatchable DERs, have the least self-adequacy and purchase expensive energy to supply their expensive loads, while they scarcely ever interrupt their loads and sell energy to the other MGs, as

Table 6: IbGC and SbER for Various Load Segments of MGs.

Segments	IbGC [MWh/year]					SbER [MWh/year]				
	MG#1	MG#2	MG#3	MG#4	MG#5	MG#1	MG#2	MG#3	MG#4	MG#5
1	0.01	0.00	0.34	1.02	0.00	0.00	0.00	0.00	0.00	0.00
2	0.77	0.00	0.49	0.62	0.00	0.00	0.00	0.00	0.00	0.00
3	11.08	0.00	4.24	11.60	0.00	0.00	0.00	0.00	0.00	0.00
4	1.42	0.00	0.72	0.74	0.00	0.00	0.00	0.00	0.00	0.00
5	—	0.00	0.47	1.07	0.00	—	0.00	0.00	0.00	0.00
6	—	0.01	0.45	0.41	0.00	—	0.81	0.00	0.00	1.02
7	—	0.00	—	0.00	0.00	—	3.42	—	0.00	6.17

measured by IbGC. These indices, in fact, indicate the imbalances and improper allocation of DERs w.r.t. the load demands and load types for each MG relative to the other MGs. Several factors can impact these two indices, e.g., the overall adequacy of the system, the self-adequacy of the MGs, and the type of loads and DERs. Accordingly, these indices are beneficial for the design and extension of MMG systems.

6. Concluding Remarks

This paper developed an adequacy assessment framework for CPMMG distribution networks, taking the device-level failures of cyber components into account. To reach this purpose, after exemplifying such a system and identifying a possible scenario for the consequence of failure of cyber components on a CPMMG, a method based on the SMCS together with the scheduling strategies suitable for investigating the system's adequacy was proposed. The reliability indices in a CPMMG largely depend on the failure and repair rates of the components. Unfortunately, there is no documented work providing suitable data on these rates for cyber system components, and there are large differences in the failure and repair rates used in various research studies. Therefore, some of the numerical results of this study that are influenced by these rates largely cannot imply general conclusions; however, some important results are robust to the changes in failure and repair rates to a high degree. Firstly, the most critical components in the cyber system—influencing the system's adequacy—are the main controllers, viz., the DMS and MGCCs. Therefore, backup controllers, or the capability to shift to a distributed control system when required, can significantly decrease the impact of cyber component failures on adequacy. Moreover, it has been shown that the proper deployment of the load controller can substantially improve the system's adequacy by interrupting the loads with lower interruption costs when there is an energy deficit in the system. The results also showed that the failure of load controllers has almost no impact on the adequacy indices. In addition, the results indicated that the internal protection and backup supply improve the system's adequacy significantly. It was also shown that the hidden failures are almost the only failures in the

FLISR process that degrade the system's reliability. Finally, two new indices—IbGC & SbER—were proposed and analyzed, and their benefits were proven for system design. This research can help the power system planner to analyze and design CPMMGs more efficiently. As a general conclusion, note that the adverse impact of cyber failures of control and protection systems can be effectively mitigated by a proper design. Therefore, it is suggested to consider the reliability indices as an important metric during the design phase.

Even though the focus of this paper has been on long-term reliability, i.e., adequacy, it is also essential to take into account the other impacts of cyber malfunctions— the most important factor being the time delay—on the dynamic and short-term reliability of these systems. In addition, the designed cyber system in this study is mostly based on fiber optics. Employing other technologies such as 5G can also be considered as a future research direction. Assessing the impact of monitoring systems on system adequacy is also another relevant topic for future research. Finally, developing an analytical approach for such a system could provide faster problem-solving.

Declaration of Competing Interest

The authors declare that they have no known competing financial interests or personal relationships that could have appeared to influence the work reported in this paper.

Acknowledgement

Appendix

An algorithm that can carry out the same task as the optimization problem **MGCC–P2(A)** is explained in this section. This algorithm for islanded MG $m \in \mathcal{M}$ at time period $t \in \mathcal{T}^{\text{ini}}$ is as follows:

$\boxed{\textbf{2.I}}$ If
$$\underbrace{L_{mt}^{\text{tot}} - (\bar{\mathcal{P}}_{mt}^{\text{w}} \cdot \phi_{mt}^{\text{w}} + \bar{\mathcal{P}}_{mt}^{\text{pv}} \cdot \phi_{mt}^{\text{pv}})}_{\zeta_{mt}} + \overset{\bullet}{\mathcal{P}}_{mt}^{\text{ch}} \leq 0, \tag{24}$$

where

$$\overset{\bullet}{\mathcal{P}}_{mt}^{\text{ch}} = \min \left[\bar{\mathcal{P}}_m^{\text{ch}}, \left(\bar{c}_m^{\text{ess}} - c_{m,t-1}^{\text{ess}} \right) / \left(\eta_m^{\text{ch}} \cdot d_t \right) \right] \cdot \phi_{mt}^{\text{ess}}, \tag{25}$$

and L_{mt}^{tot} is the total load of MG m by taking the failed transformers into account. In this situation, the diesel generators are set to the minimum possible production, which is zero here, and

36

the ESS will be charged to the maximum possible amount $\overset{\bullet}{\mathcal{P}}^{\text{ch}}_{mt}$; the generation of the renewable resources is reduced to meet the power balance constraint $\zeta_{mt} + \overset{\bullet}{\mathcal{P}}^{\text{ch}}_{m} = 0$, and there is no load shedding $\left(\mathcal{P}^{\text{ls}}_{mrt} = 0 : \forall_r \in \mathcal{R}_m \right)$.

2.II   Else if

$$\zeta_{mt} + \overset{\bullet}{\mathcal{P}}^{\text{ch}}_{mt} \leq \sum_{d \in \mathcal{D}_m} \bar{\mathcal{P}}^{\text{de}}_{md} \cdot \phi^{\text{de}}_{mdt}, \tag{26}$$

then

$$\mathcal{P}^{\text{ch}}_{mt} = \overset{\bullet}{\mathcal{P}}^{\text{ch}}_{mt}, \tag{27}$$

$$\left(\mathcal{P}^{\text{de}}_{mdt} : \forall_d \in \mathcal{D}_m \right) = \arg \min \sum_{d \in \mathcal{D}_m} \mathcal{F}_{mt}(\mathcal{P}^{\text{de}}_{mdt}), \tag{28}$$

$$\text{s.t.:} \quad \sum_{d \in \mathcal{D}_m} \mathcal{P}^{\text{de}}_{mdt} \cdot \phi^{\text{de}}_{mdt} = \zeta_{mt} + \overset{\bullet}{\mathcal{P}}^{\text{ch}}_{mt}, \tag{29}$$

2.III   Else if

$$\zeta_{mt} \leq \sum_{d \in \mathcal{D}_m} \bar{\mathcal{P}}^{\text{de}}_{md} \cdot \phi^{\text{de}}_{mdt}, \tag{30}$$

then

$$\mathcal{P}^{\text{de}}_{mdt} = \bar{\mathcal{P}}^{\text{de}}_{md} \cdot \phi^{\text{de}}_{mdt} \quad \forall_d \in \mathcal{D}_m, \tag{31}$$

$$\mathcal{P}^{\text{ch}}_{mt} = \sum_{d \in \mathcal{D}_m} \bar{\mathcal{P}}^{\text{de}}_{md} \cdot \phi^{\text{de}}_{mdt} - \zeta_{mt}, \tag{32}$$

2.IV   Else if

$$\zeta_{mt} \leq \sum_{d \in \mathcal{D}_m} \bar{\mathcal{P}}^{\text{de}}_{md} \cdot \phi^{\text{de}}_{mdt} + \overset{\bullet}{\mathcal{P}}^{\text{dch}}_{m}, \tag{33}$$

where

$$\overset{\bullet}{\mathcal{P}}^{\text{dch}}_{m} = \min \left[\bar{\mathcal{P}}^{\text{dch}}_{m}, \left(c^{\text{ess}}_{m,t-1} - \underline{c}^{\text{ess}}_{m} \right) \cdot \eta^{\text{dch}}_{m} / d_t \right] \cdot \phi^{\text{ess}}_{mt}, \tag{34}$$

then

$$\mathcal{P}^{\text{dch}}_{mt} = \zeta_{mt} - \sum_{d \in \mathcal{D}_m} \bar{\mathcal{P}}^{\text{de}}_{md} \cdot \phi^{\text{de}}_{mdt}, \tag{35}$$

$$\mathcal{P}^{\text{de}}_{mdt} = \bar{\mathcal{P}}^{\text{de}}_{md} \cdot \phi^{\text{de}}_{mdt} \quad : \forall_d \in \mathcal{D}_m, \tag{36}$$

2.V   Else

$$\mathcal{P}^{\text{de}}_{mdt} = \bar{\mathcal{P}}^{\text{de}}_{md} \cdot \phi^{\text{de}}_{mdt} \quad : \forall_d \in \mathcal{D}_m, \tag{37}$$

$$\mathcal{P}^{\text{dch}}_{mt} = \overset{\bullet}{\mathcal{P}}^{\text{dch}}_{mt}, \tag{38}$$

$$\left(\mathcal{P}^{\text{ls-mg}}_{mrt} : \forall_{r \in \mathcal{R}_m} \right) = \arg \min \sum_{r \in \mathcal{R}_m} \lambda^{\text{ls-mg}}_{mrt} \cdot \mathcal{P}^{\text{ls-mg}}_{mrt}, \tag{39}$$

$$\text{s.t.:} \quad \zeta_{mt} - \sum_{d \in \mathcal{D}_m} \bar{\mathcal{P}}^{\text{de}}_{md} \cdot \phi^{\text{de}}_{mdt} - \overset{\bullet}{\mathcal{P}}^{\text{dch}}_{mt} \leq \sum_{r \in \mathcal{R}_m} \mathcal{P}^{\text{ls-mg}}_{mrt}, \tag{40}$$

$$(11) \qquad \qquad : \forall_r \in \mathcal{R}_m. \tag{41}$$

37

Note that the amount of renewable generation is set to maximum ($\mathcal{P}_{mt}^{\mathrm{w}} = \bar{\mathcal{P}}_{mt}^{\mathrm{w}} \cdot \phi_{mt}^{\mathrm{w}}; \mathcal{P}_{mt}^{\mathrm{pv}} = \bar{\mathcal{P}}_{mt}^{\mathrm{pv}} \cdot \phi_{mt}^{\mathrm{pv}}$) for **2.II**–**2.V**. Some remarks about this algorithm should be made. If there is only one diesel engine in the MG, the optimization problem (28) is not needed. In this algorithm, the ESS is used to serve the loads with minimum interruption cost. This is equivalent to mathematical formulation problem **MGCC–P2(A)** with λ^{ess} equal to the minimum interruption cost in the MG. For the other values of λ^{ess}, some modifications are needed. Note that after this process, the SOC of the ESS c_{mt}^{ess} is updated using (4).

References

[1] M. Shi, H. He, J. Li, M. Han, C. Jia, Multi-objective tradeoff optimization of predictive adaptive cruising control for autonomous electric buses: A cyber-physical-energy system approach, Applied Energy 300 (2021) 117385. doi:https://doi.org/10.1016/j.apenergy.2021.117385.

[2] W. Wang, T. Hong, N. Li, R. Q. Wang, J. Chen, Linking energy-cyber-physical systems with occupancy prediction and interpretation through wifi probe-based ensemble classification, Applied Energy 236 (2019) 55–69. doi:https://doi.org/10.1016/j.apenergy.2018.11.079.

[3] B. Falahati, Y. Fu, L. Wu, Reliability assessment of smart grid considering direct cyber-power interdependencies, IEEE Trans. Smart Grid 3 (3) (2012) 1515–1524. doi:10.1109/TSG.2012.2194520.

[4] M. H. Rehmani, M. Reisslein, A. Rachedi, M. Erol-Kantarci, M. Radenkovic, Integrating renewable energy resources into the smart grid: Recent developments in information and communication technologies, IEEE Trans. Ind. Informat. 14 (7) (2018) 2814–2825. doi:10.1109/TII.2018.2819169.

[5] I. A. Tøndel, J. Foros, S. S. Kilskar, P. Hokstad, M. G. Jaatun, Interdependencies and reliability in the combined ICT and power system: An overview of current research, Applied Computing and Informatics 14 (1) (2018) 17–27.

[6] B. Falahati, Y. Fu, A study on interdependencies of cyber-power networks in smart grid applications, in: 2012 IEEE PES Innovative Smart Grid Technologies (ISGT), 2012, pp. 1–8. doi:10.1109/ISGT.2012.6175593.

[7] B. Falahati, Y. Fu, Reliability assessment of smart grids considering indirect cyber-power interdependencies, IEEE Trans. Smart Grid 5 (4) (2014) 1677–1685. doi:10.1109/TSG.2014.2310742.

[8] A. Hassani Ahangar, H. A. Abyaneh, G. Gharepetian, Negative effects of cyber network (control, monitoring, and protection) on reliability of smart grids based on DG penetration, in: 2015 5th

International Conference on Computer and Knowledge Engineering (ICCKE), 2015, pp. 54–60. doi:10.1109/ICCKE.2015.7365861.

[9] A. Hassani, B. Vahidi, H. Abyaneh, Evaluating smart grid reliability based on impacts of cyber (control, monitoring and protection) network and its different topologies, International Journal of System Assurance Engineering and Management 9 (07 2018). doi:10.1007/s13198-018-0730-0.

[10] H. Hashemi-Dezaki, S. M. M. Agah, H. Askarian-Abyaneh, H. Haeri-Khiavi, Sensitivity analysis of smart grids reliability due to indirect cyber-power interdependencies under various DG technologies, DG penetrations, and operation times, Energy Conversion and Management 108 (2016) 377–391. doi:https://doi.org/10.1016/j.enconman.2015.10.082.

[11] H. Hashemi-Dezaki, H. Askarian-Abyaneh, A. Shams-Ansari, M. DehghaniSanij, M. A. Hejazi, Direct cyber-power interdependencies-based reliability evaluation of smart grids including wind/solar/diesel distributed generations and plug-in hybrid electrical vehicles, International Journal of Electrical Power & Energy Systems 93 (2017) 1–14. doi:https://doi.org/10.1016/j.ijepes.2017.05.018.

[12] W. Zhu, M. Han, J. V. Milanović, P. Crossley, Methodology for reliability assessment of smart grid considering risk of failure of communication architecture, IEEE Trans. Smart Grid 11 (5) (2020) 4358–4365. doi:10.1109/TSG.2020.2982176.

[13] G. Cao, W. Gu, P. Li, W. Sheng, K. Liu, L. Sun, Z. Cao, J. Pan, Operational risk evaluation of active distribution networks considering cyber contingencies, IEEE Trans. Ind. Informat. 16 (6) (2020) 3849–3861. doi:10.1109/TII.2019.2939346.

[14] W. Liu, Q. Gong, H. Han, Z. Wang, L. Wang, Reliability modeling and evaluation of active cyber physical distribution system, IEEE Trans. Power Syst. 33 (6) (2018) 7096–7108. doi:10.1109/TPWRS.2018.2854642.

[15] W. Liu, Z. Lin, L. Wang, Z. Wang, H. Wang, Q. Gong, Analytical reliability evaluation of active distribution systems considering information link failures, IEEE Transa. on Power Syst. 35 (6) (2020) 4167–4179. doi:10.1109/TPWRS.2020.2995180.

[16] D. Lin, Q. Liu, Z. Li, G. Zeng, Z. Wang, T. Yu, J. Zhang, Elaborate reliability evaluation of cyber physical distribution systems considering fault location, isolation and supply restoration process, IEEE Access 8 (2020) 128574–128590. doi:10.1109/ACCESS.2020.3007477.

[17] X. Zhou, Z. Yang, M. Ni, H. Lin, M. Li, Y. Tang, Analysis of the impact of combined information-physical-failure on distribution network CPS, IEEE Access 8 (2020) 44140–44152. doi:10.1109/ACCESS.2020.2978113.

[18] C. Wang, T. Zhang, F. Luo, F. Li, Y. Liu, Impacts of cyber system on microgrid operational reliability, IEEE Trans. Smart Grid 10 (1) (2019) 105–115. `doi:10.1109/TSG.2017.2732484`.

[19] J. Guo, T. Zhao, W. Liu, J. Zhang, Reliability modeling and assessment of isolated microgrid considering influences of frequency control, IEEE Access 7 (2019) 50362–50371. `doi:10.1109/ACCESS.2019.2909153`.

[20] M. Aslani, H. Hashemi-Dezaki, A. Ketabi, Reliability evaluation of smart microgrids considering cyber failures and disturbances under various cyber network topologies and distributed generation's scenarios, Sustainability 13 (10) (2021). `doi:10.3390/su13105695`.

[21] M. Aslani, J. Faraji, H. Hashemi-Dezaki, A. Ketabi, A novel clustering-based method for reliability assessment of cyber-physical microgrids considering cyber interdependencies and information transmission errors, Applied Energy 315 (2022) 119032. `doi:https://doi.org/10.1016/j.apenergy.2022.119032`.

[22] X. Yang, Y. Wang, Y. Zhang, W. Yao, J. Wen, Impact analysis of cyber system in microgrids: Perspective from economy and reliability, Int. J. Electr. Power Energy Syst. 135 (2022) 107422. `doi:https://doi.org/10.1016/j.ijepes.2021.107422`.

[23] M. Barani, V. V. Vadlamudi, P. E. Heegaard, Reliability analysis of cyber-physical microgrids: Study of grid-connected microgrids with communication-based control systems, IET Generation, Transmission & Distribution 15 (4) (2021) 645–663. `doi:https://doi.org/10.1049/gtd2.12049`.

[24] S. P. Chowdhury, Microgrids and Active Distribution Networks, Energy Engineering, Institution of Engineering and Technology, 2009.

[25] M. Barani, J. Aghaei, M. A. Akbari, T. Niknam, H. Farahmand, M. Korpås, Optimal partitioning of smart distribution systems into supply-sufficient microgrids, IEEE Trans. Smart Grid (3) (2019).

[26] A. Kargarian, B. Falahati, Y. Fu, M. Baradar, Multiobjective optimal power flow algorithm to enhance multi-microgrids performance incorporating ipfc, in: 2012 IEEE General Meeting, 2012, pp. 1–6.

[27] L. Fusheng, L. Ruisheng, Z. Fengquan, Chapter 2 - Composition and classification of the microgrid, in: L. Fusheng, L. Ruisheng, Z. Fengquan (Eds.), Microgrid Technology and Engineering Application, Academic Press, Oxford, 2016, pp. 11 – 27. `doi:https://doi.org/10.1016/B978-0-12-803598-6.00002-4`.

[28] R. He, S. Yang, J. Deng, T. Feng, L. L. Lai, M. Shahidehpour, Reliability analyses of wide-area protection system considering cyber-physical system constraints, IEEE Transactions on Smart Grid 12 (4) (2021) 3458–3467. `doi:10.1109/TSG.2021.3060941`.

[29] M. M. Eissa, A novel centralized wide area protection "cwap" in phase portrait based on pilot wire including phase comparison, IEEE Transactions on Smart Grid 10 (3) (2019) 2671–2682. `doi:10.1109/TSG.2018.2808207`.

[30] R. Billinton, P. Wang, Teaching distribution system reliability evaluation using monte carlo simulation, IEEE Transactions on Power Systems 14 (2) (1999) 397–403. `doi:10.1109/59.761856`.

[31] Online: https://www.renewables.ninja, accessed january 2020.

[32] H. Farzin, M. Fotuhi-Firuzabad, M. Moeini-Aghtaie, Reliability studies of modern distribution systems integrated with renewable generation and parking lots, IEEE Trans. Sustain. Energy (1) (2017) 431–440. `doi:10.1109/TSTE.2016.2598365`.

[33] A. Churkin, Stability analysis in coalitional games for cross-border power interconnecting planning, Ph.D. thesis, Skolkovo Institute of Science and Technology (2020).

[34] W. Li, et al., Reliability assessment of electric power systems using Monte Carlo methods, Springer Science & Business Media, 2013.

[35] R. Billinton, R. N. Allan, Power-system reliability in perspective, Electronics and Power 30 (3) (1984) 231–236. `doi:10.1049/ep.1984.0118`.

[36] P. J. Balducci, J. M. Roop, L. A. Schienbein, J. G. DeSteese, M. R. Weimar, Electric power interruption cost estimates for individual industries, sectors, and U.S. economy, Pacific Northwest National Laboratory Report (Feb. 2002). `doi:10.2172/926127`.

[37] M. Saleh, Y. Esa, M. E. Hariri, A. Mohamed, Impact of information and communication technology limitations on microgrid operation, Energies 12 (15) (2019) 2926.